

54

PURIFICATION OF RECOMBINANT PROTEINS

by

GEORGE CLIFFORD RUTT

B.S., University of Arizona
(1985)

M.A., University of Alaska
(1988)

SUBMITTED IN PARTIAL FULFILLMENT
OF THE REQUIREMENTS
FOR THE DEGREE OF
MASTER OF SCIENCE
at the
MASSACHUSETTS INSTITUTE OF TECHNOLOGY
December, 1996
[February, 1997]

Signature of Author _____
Department of Chemical Engineering
December 16, 1996

Certified by _____ Thesis Supervisor

Accepted by _____
Chairman, Departmental Committee
on Graduate Students

MASSACHUSETTS INSTITUTE
OF TECHNOLOGY

APR 28 1997

LIBRARIES

ABSTRACT

This project involved the design of a scaled-up process for the purification of a novel class of recombinant proteins, silk-elastin like proteins (SELP), which are block copolymers of the repeat amino acid sequence of silk (GAGAGS) and elastin (GVGVP). To facilitate process development, an HPLC assay for SELP was developed utilizing hydrophobic interaction chromatography which is less tedious and more quantitative than the existing assay. The purification protocol consists of flocculating cellular debris and anionic impurities, including nucleic acids, with a cationic polymer, followed by two sequential ammonium sulfate precipitations. This results in a 99.+ % purity of the SELP biopolymer. Two polymers, polyethyleneimine (PEI), and poly(dimethyldiallyl ammonium chloride) (PDMDAAC), were studied for impurity removal and flocculation properties. Optimal impurity removal correlated with optimal settling, and were found to be a function of pH and polymer concentration. The optimal condition for flocculation by PEI was found to be at a pH between 8 and 9, and a PEI concentration of 0.4 wt/vol % for lysate produced from 50 g/L dcw cells. PDMDAAC was determined to have significantly improved impurity removal and particulate settling characteristics at pH values above 11. A continuous polymer flocculation process is proposed, utilizing static mixers with continuous stirred tank particle aging, followed by centrifugation. The two sequential ammonium sulfate precipitation steps of SELP were characterized. Operating at 20% saturation (~0.8 M ammonium sulfate) is sufficient to precipitate three separate SELP species at yields greater than 99%. The ammonium sulfate precipitates have a spherical and highly deformable morphology. Precipitates from the second ammonium sulfate step are highly adhesive, suggesting the final design should incorporate features to avoid large losses during processing. In addition, HPLC-based techniques for characterizing product variability were developed.

ACKNOWLEDGMENTS

I would like to thank my thesis advisor, Professor Daniel Wang, for helping to advance both this thesis, and my own professional development during my tenure here at MIT. I am grateful for the many paths that his guidance has opened to me. Dr. Franco Ferrari and the people at Protein Polymer Technologies in San Diego provided raw materials, technical advice, and moral support for this project. I look forward with anticipation to interacting further with them. Communications with Rich Mathies at Alfa Laval Corporation helped me understand aspects of industrial centrifugation. Special thanks go to Jerry Sweeney, who assisted in the torturous task of final editing.

Communications with the people of our research group proved invaluable for maintaining an enjoyable stay here. S. Meier, R. Balcarcel, J. Goswami, B. Follstad, G. Nyberg, A. Lamouse-Smith, M. Shelikoff, T. Simpson, J. Gargano, and S. Gu, will sorely be missed for the many shared technical and philosophical discourses. Special thanks go to Dr. John Chung, whose always available comments assisted in producing a better product. Additionally, Dr. Brian Kelley, and Eric Scharin provided helpful insight into industrial operations.

Personal acknowledgments must go to people too numerous to mention here. I have been blessed with friends and family that support my efforts. Singling out a few individuals may only diminish the contributions of others. To all of you, I thank you deeply.

TABLE OF CONTENTS

LIST OF FIGURES	6
LIST OF TABLES	8
I. INTRODUCTION	9
II. OBJECTIVE	13
III. BACKGROUND	13
A. Silk Elastin Like Proteins (SELP)	13
B. Small-Scale Purification of SELP	15
C. Literature Survey on Precipitation	22
C.1 Precipitate Recovery	23
C.2 Formation of Precipitates by Polyelectrolytes	25
C.3 Formation of Precipitates by Salting-Out	29
IV. MATERIALS AND METHODS	43
A. Assay Development and SELP8K Characterization	44
B. Polyelectrolyte Precipitation	49
C. Ammonium Sulfate Precipitation	52
V. RESULTS AND DISCUSSION	56
A. Characterization of SELP8K	56
B. Polymer Flocculation	
B.1. Polyethyleneimine Precipitation	63
B.2. Poly(dimethyldiallyl ammonium chloride) Precipitation	68
B.3. Characterization of Solid-Liquid Separation	72

C.	Ammonium Sulfate Precipitation of SELP Proteins	80
C.1.	Effect of Temperature on SELP Solubility	80
C.2.	Effect of Impurities on Solubility	84
C.3.	Characterization of Solid Precipitate	87
VI.	PROCESS SYNTHESIS	94
A.	Cell Harvesting	97
B.	Cell Disruption	99
C.	Polymer Precipitation of Lysate	101
D.	Ammonium Sulfate Precipitation	108
E.	Diafiltration/Ultrafiltration	112
F.	Endotoxin Removal	113
G.	Product Formulation	114
VII.	BIBLIOGRAPHY	115

LIST OF FIGURES

Figure I:	SELP8K Primary Amino Acid Sequence	14
Figure II:	Small Scale SELP Purification Protocol	17
Figure III:	Batch Scheduling of SELP Purification	18
Figure IV:	Process Volumes for Large Scale SELP Purification	20
Figure V:	Precipitation Behavior of Two Hypothetical Proteins	33
Figure VI:	Kinetic Competition Between Particle Nucleation and Growth	36
Figure VII:	Hydrophobic Interaction Chromatography Behavior of Different SELP Species	45
Figure VIII.	Immobilized Metal Affinity Chromatography of SELP8K	57
Figure IX.	Cation Exchange Chromatography of SELP8K and Results from Reinjection of Collected Peaks	59
Figure X.	Cation Exchange Chromatography of Cyanogen Bromide Treated SELP8K	60
Figure XI.	Size Exclusion Behavior of SELP8K	62
Figure XII.	Effect of Protein Concentration on the Size Exclusion Behavior of SELP8K	63
Figure XIII:	Analysis of PEI Treated Lysate Supernatant, pH 7	64
Figure XIV:	Effect of pH and PEI Concentration on the Removal of Protein Impurities from <i>Escherichia coli</i> Derived Lysate	67

Figure XV:	Effect of pH and PDMDAAC Concentration on the Removal of Protein Impurities from <i>Escherichia coli</i> Derived Lysate	69
Figure XVI:	Potential Mechanism of the pH Effect on PEI Flocculation	75
Figure XVII:	Effect of Mixing and PEI Addition Rate on Settling Behavior	77
Figure XVIII:	Comparison of the Extent of Settling of Lysate Treated with PEI and PDMDAAC Polymers	78
Figure XIX:	Effect of Temperature on the Salting-out Curves for Prepurified SELP8K, SELP0K, and SELP0K-CS1	81
Figure XX:	Effect of Lysate Impurities on the Salting-out Curves for SELP	84
Figure XXI:	Morphology of SELP0K Particles formed from the Supernatant of Polymer Treated Lysate	89
Figure XXII:	Morphology of SELP0K Particles formed from Purified Sources	90
Figure XXIII:	SELP Purification Process Flowsheet	95
Figure XXIV:	SELP Purification Process Flow Diagram	96
Figure XXV:	Proposed Configuration for Polyethyleneimine Flocculation of Lysate	104
Figure XXVI:	Fed Batch Reactor for Ammonium Sulfate Precipitation	109
Figure XXVII:	Schematic of a Typical Dia/ultrafiltration Operation	113

LIST OF TABLES

Table I:	Protein Purification Options	11
Table II:	Cationic Polymer Characteristics	28
Table III:	Concentration of Ammonium Sulfate at the Apex of the SELP Elution Peak	46
Table IV:	SELP8K Yields at Various Conditions	70
Table V:	Settling of PEI Treated Lysate, Measured by Visual Observation at 15 minutes	73
Table VI:	Effect of Temperature on Parameters for the Cohn Equation for Different SELP Species	82
Table VII:	Parameters for the Cohn Equation for Different SELP Species Precipitated from the Supernatant of PEI Treated Lysate	85

I. INTRODUCTION

The recent development of recombinant DNA technology has enabled the production of a wide variety of polypeptide biopolymers in biochemical fermentation processes. The design of processes to purify these new biopolymers has relied for the most part on the scale-up of laboratory protocols. Batch processes are predominant, in part because of the batch nature of producing proteins by fermentation, and also due to the cost of reagents associated with potential continuous processes. Unlike processes involving small molecules, whose physical and chemical attributes can be predicted accurately, the ability to predict protein purification operations from first principles is untenable. This is due to the inherently complex nature of proteins, where subtle conformational changes can have tremendous impact on their physical characteristics. As a result, experiments at progressively larger scales of operation are essential to approach a final optimized process.

Separation of a specific protein from cellular material consisting of carbohydrates, proteins, lipids, DNA, RNA, and assorted organic and inorganic moieties is inherently challenging. Often the protein of interest has characteristics similar to other components in the cell resulting in a

difficult separation. The high purity required for biomedical applications often results in low yields, which translates to higher costs. Indeed, purification related cost can be up to 80-90% of the total production costs (Harrison, 1994). To minimize this cost, purification operations should be designed to take full advantage of any differential properties of the protein of interest. As shown in Table I, a number of purification operations exist to differentiate between the protein of interest and contaminants.

Table I: Protein Purification Options

<u>Differential Biopolymer Characteristic</u>	<u>Purification Operation</u>
Ionic Charge	Ion exchange chromatography Isoelectric precipitation
Hydrophobicity	Reversed phase chromatography Hydrophobic interaction chromatography Differential precipitation Liquid-liquid extraction
Specific binding site	Affinity chromatography Immobilized antibody Immobilized ligand or mimic Immobilized metal
Size	Gel permeation chromatography Dialysis/Diafiltration

For laboratory scale purification, protocols involving many steps can be

carried out in an acceptable time period. The overall yield of the process is not as important as the ability to produce an acceptable amount of pure product. At larger scales, low yields translate directly into decreased profitability. Poor yields often result upon scale-up for commercial production as a result of inherent inefficiencies of some large scale processes. Larger processing volumes also often necessitate longer processing times which may increase product degradation.

Some purification operations are more easily scaled up than others. For instance, chromatography based on binding and elution is scaled up by simply keeping the linear velocity of the process fluid through the column constant and scaling the adsorption capacity of the column to the amount of protein in the fluid. Ultrafiltration/diafiltration operations are scaled up by keeping the fluid dynamics considerations similar (for instance shear rate at the membrane surface) and the pressure difference across the membrane constant, which results in a transmembrane flux which is independent of scale. The total filtration area is then determined by the volume of fluid processed.

In contrast, the performance (yield and flowrate) of centrifugation suffers

during scale-up. Laboratory centrifuges produce higher relative g force than continuous equipment, resulting in a tighter pellet with less entrained impurities. Solids separation is accomplished by simply decanting the supernatant from the pellet. Solids removal in commercial scale centrifuges is accomplished by either disassembling the centrifuge and manually cleaning the machine, or by a continuous discharge mechanism, which results in a particulate sludge with a necessarily higher liquid content to avoid plugging the discharge mechanism. As a result, a decreased yield of liquid components and a less pure particulate product are observed. Furthermore, as will be discussed in detail later, the separability and purity of the particulate phase in precipitation processes is often highly dependent on scale-sensitive variables such as precipitant addition rate, the rate of mixing, and reactor configuration (Fisher and Glatz, 1986; Bell and Dunnill, 1982). These examples illustrate some of the differences between large-scale and small-scale operation and serve to emphasize the importance of considering scale-up considerations in process design. The challenge for the chemical engineer is to apply a firm understanding of biochemical phenomena and separation technology to design an industrial process that produces an acceptable product in an economically feasible manner.

II. OBJECTIVE

The objective of this thesis is to determine operating parameters for a large-scale (~1 Metric ton/year) process to purify an *Escherichia coli* produced biopolymer based on the repeat sequences of silk and elastin. An existing laboratory protocol is optimized, and then used as the basis for this design. Expected deviations from the laboratory scale results are discussed, and when applicable, solutions are proposed.

III. BACKGROUND

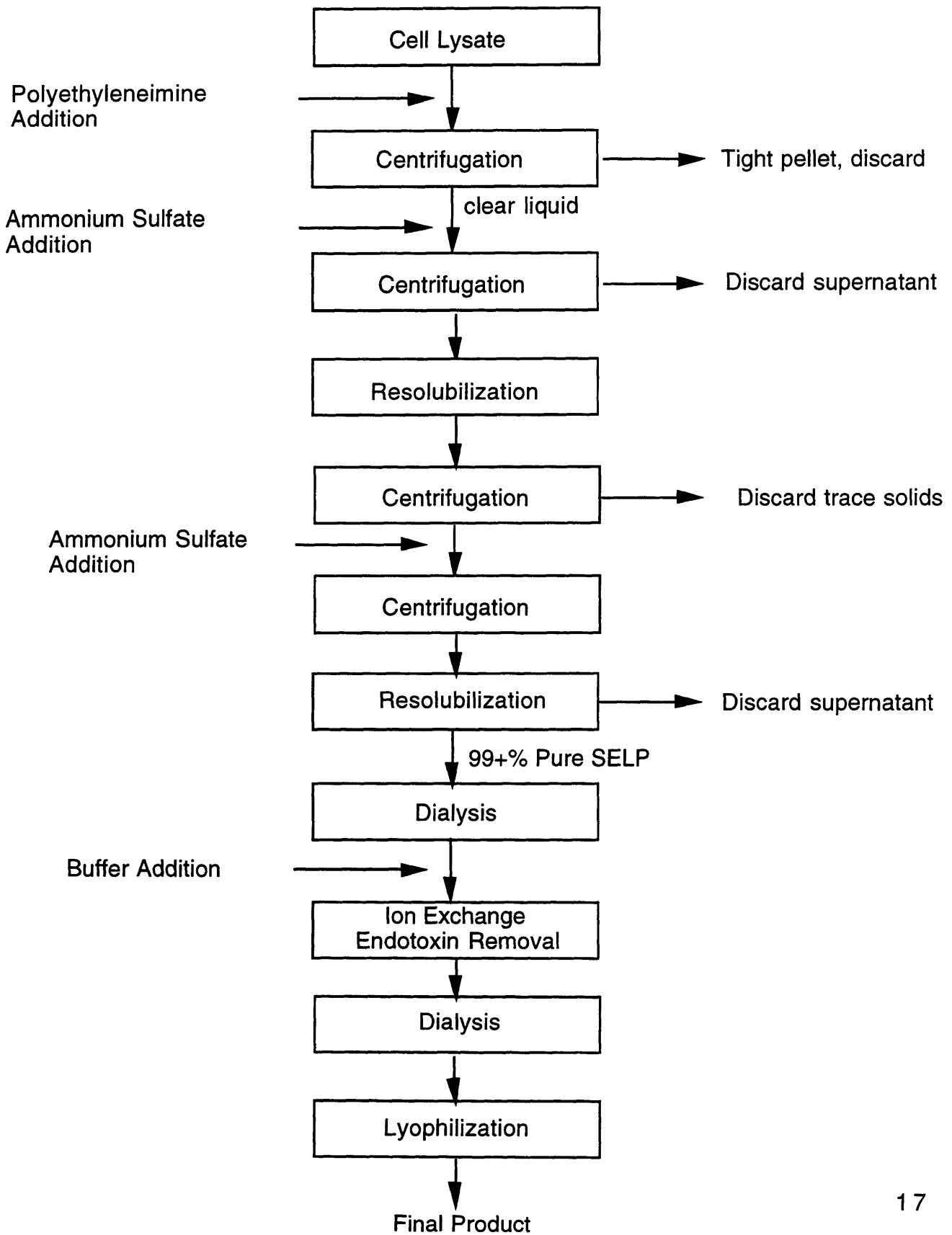
Silk Elastin Like Proteins (SELP): A new material has recently been produced using recombinant DNA technology to incorporate the repeat amino acid sequence of silk (GAGAGS) and elastin (GVGVP) into a polypeptide copolymer. The sequence of one of these constructs, designated SELP8K, is shown in Figure I. In addition to SELP8K, two other SELP proteins were used for this research, SELP0K and SELP0K-CS1. The main difference between SELP0K and SELP8K is that whereas SELP8K has four silk units for every eight elastin units, SELP0K has two silk units for every eight elastin units. SELP0K-CS1 has the same silk to elastin ratio as SELP0K with an additional

which can stretch under tension to many times the original length and return to its original conformation when the tension is released. By altering the relative proportions of the elastin and silk repeat units, a family of biomaterials have been made which have a range of characteristics such as solubility and fiber-forming ability (Cappello, 1994). The immunologically inert behavior of these materials has been demonstrated (F. Ferrari, personal communication), suggesting potential application as a biomaterial. Introducing specific residues in the sequence, for instance amino acids which confer *in vivo* protease susceptibility, allows for the ability to tailor properties such as adhesiveness or bioresorbability to a specific application. Presently one such construct is being evaluated as a tissue sealant and adhesive. The broad market potential of such a use, should this material prove beneficial, will generate a demand of metric tons per year, necessitating large-scale manufacturing technology.

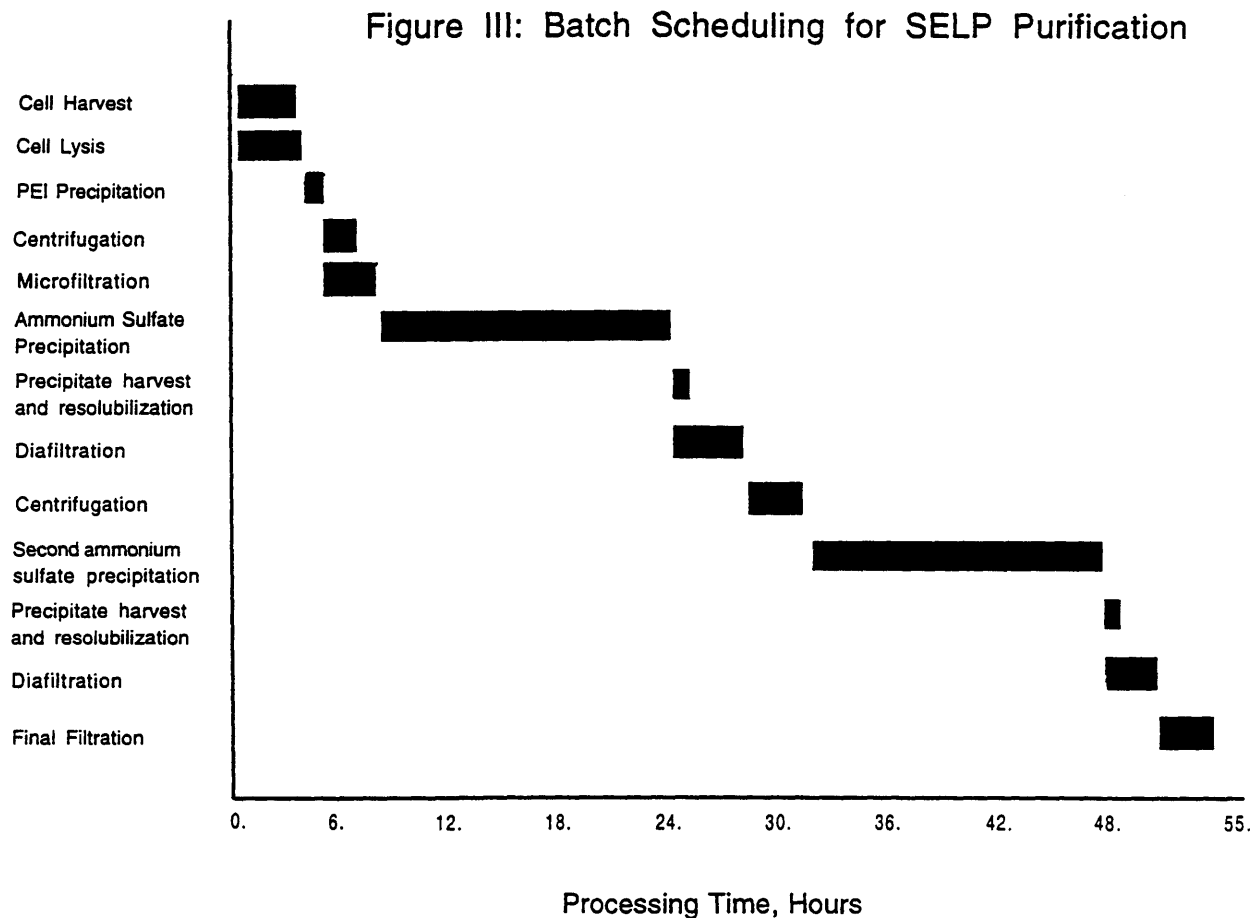
Small-Scale Purification of SELP: The potential biomedical applications for SELP require exceptionally pure material which is endotoxin free, and devoid of cytotoxicity. The amino acid sequence of SELP8K, shown in Figure I, indicates two obvious characteristics which are

amenable to purification process design. First, SELP has a low number of negative amino acids, suggesting that anion exchange techniques can be utilized to remove negative impurities from the process stream leaving the SELP unbound. Second, the amino acid composition is dominated by the hydrophobic residues alanine, glycine, valine, and proline, indicating that separation techniques based on hydrophobicity will be effective. The current protocol, shown in Figure II, utilizes these characteristics to produce multigram amounts of material that passes the purity requirements. The process consists of cell separation by centrifugation, followed by cell disruption by homogenization. Cellular debris and negatively charged impurities are precipitated by the cationic polymer polyethyleneimine, and separated by centrifugation. SELP is purified from the resulting clear supernatant by ammonium sulfate precipitation. The precipitated SELP is allowed to settle overnight, and the mother liquor is decanted. The next day the SELP precipitate is redissolved and centrifuged to remove insoluble impurities. The ammonium sulfate step is repeated, and the resulting solution diafiltered to exchange the buffer, filtered with a 0.2 μm membrane, and passed through an endotoxin-removing anion exchange column. The chromatography elution buffer is removed by diafiltration and the solution is sterile filtered and lyophilized.

Figure II: Small-Scale SELP Purification Protocol



Analysis of the Scaled-up Laboratory Protocol: For the design of a large-scale production process the design basis will be a scaled-up laboratory process. The scheduling for this process is shown in Figure III in the form of a Gantt scheduling chart.



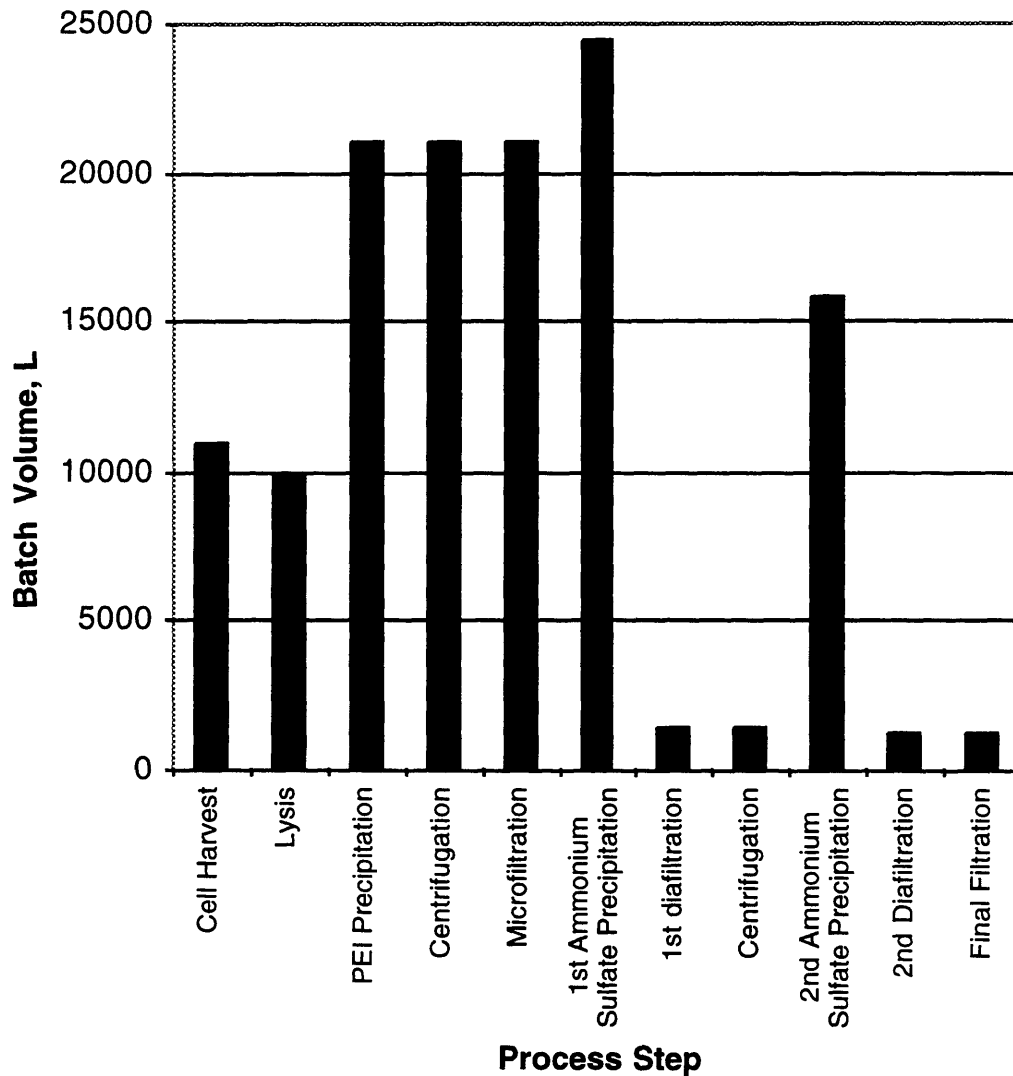
The basis of the scheduling is a direct scale-up of the laboratory protocol, with steps leading up to the overnight settling occurring in an eight-hour work day. While this minimizes the labor costs by using day-shift workers

for most of the processing, it is not optimized with respect to production costs as the high capital costs of the equipment and facilities can best be utilized by continuous operations at maximal efficiency. The scheduling chart shows the two overnight settling steps associated with the ammonium sulfate precipitation to be rate limiting. Increasing the throughput of the plant would require multiple settling tanks, or replacing the gravity settling steps with centrifugal separation, at the cost of multiple shift operation. For small-scale manufacturing, the extra costs associated with continuous operations are not desirable, but for large-scale operations, with associated high capital costs, 24 hour operation is necessary for full equipment utilization. Thus the use of centrifugal recovery of the ammonium sulfate precipitate should be examined to reduce the batch turnaround time.

In addition to processing times, process volumes are important in determining overall costs. Higher volumes require more expensive equipment to complete processing within a given time. Additionally, longer processing times associated with larger volumes can increase protein degradation. Shown in Figure IV are volumes that the required equipment must process to produce 1000 Kg/yr (Design Basis: 1.5 g/L SELP in

fermentation broth, 60% overall yield, 100 batches per year).

Figure IV : Process Volumes for Large Scale SELP Purification



Mixing of the polyethyleneimine solution results in a large increase in volume. For the laboratory scale workups, a 1:1 volume addition of 0.8 wt% PEI is used, bringing the final PEI concentration to 0.4 wt%. A more

concentrated PEI solution could be used, which would reduce the volume of all subsequent steps up to the first ammonium sulfate precipitation. However, a more concentrated polymer-lysate suspension would also decrease yield due to a higher content of SELP in the entrained liquid of subsequent separations. The current protocol is to perform the second ammonium sulfate precipitation from a dilute 1 mg/ml SELP solution, which is necessary to eliminate cytotoxic impurities from the product.

Concluding the scale-up analysis, minimizing the process volume increase at the PEI step would lower processing costs, at the expense of a decreased yield. Alternatively, a continuous process for the PEI flocculation step should be evaluated, as this will minimize the effect of the larger process volumes associated with higher dilutions. Furthermore, centrifugation of the ammonium sulfate precipitate should be evaluated for improving the process throughput. A continuous process for precipitate formation and recovery should also be evaluated, for the same reason given for the PEI flocculation step above. As previously mentioned, scale-up of both precipitation and centrifugation are often plagued with low yields and/or low purity (Bell, 1983; Rothstein, 1993). The following section will provide a technical basis for addressing these potential problems.

Literature Survey on Precipitation: The reasons for utilizing precipitation in a purification process are to reduce the process volume (concentration) and enrich the protein of interest (purification). To realize the benefits from precipitation the solid should also be easily recovered. In a recent comprehensive review (Rothstein 1994), it was stated that the objectives of the precipitation process, in order of priority, are:

1. Maximum separation of the solute of interest, in its native state, from other solutes (high selectivity);
2. Minimum coprecipitation;
3. Large granular particles;
4. Minimum amount of mother liquor; and
5. Maximum difference in particle density relative to that of the solution.

The purity of the precipitate is determined by items 1, 2, and 4 above, whereas the separability by centrifugation is primarily determined by factors 3 and 5. Separation of protein precipitates is usually performed by centrifugation because filtration is typically plagued by poor filterability

of the solid and by membrane fouling. This section will address the centrifugal separation of particles, followed by an analysis of the effect that particulate formation has on purity and separability. The reader is referred to the reviews of Rothstein (1993) and Bell and Dunnill (1983) for a more general treatment of precipitation phenomena.

Precipitate Recovery: A solid spherical particle will settle under the influence of gravity with a velocity given by the Stokes relationship:

$$(1) \quad V_g = d_p^2 g (\rho_p - \rho_f) / 18\mu$$

Where ρ_p , ρ_f = density of the particle and fluid respectively, μ = viscosity of the fluid, d_p = particle diameter, and g = gravitational acceleration. This equation is derived for viscous flow, i.e., a Reynolds number < 1 , and for low particle concentrations where hindered settling is not a factor. For particle separation in a centrifugal field, the same behavior holds, but the gravitational acceleration g is replaced by the angular acceleration $\omega^2 r$, where ω is the angular velocity and r is the radial position of the particle. The squared relationship between settling velocity and particle size make this variable dominant in determining centrifuge performance.

The design equation for continuous centrifugation is derived by utilizing the

concept of the limiting particle, which is the smallest particle that one hopes to separate. Centrifuge throughput is then given by:

$$(2) \quad Q = 2V_g\Sigma$$

Where Q is the flowrate through the centrifuge, V_g is the gravity settling velocity of the limiting particle, and Σ is a function of the centrifuge type and geometry. The quantity Σ is equivalent to the area of a gravity settling apparatus with the same throughput as the centrifuge. Equations for Σ are given in the review of Axelson (1985) for various commercially available centrifuges.

The assumptions needed to derive these equations (e.g., nonhindered settling, spherical particles of uniform density) are rarely encountered in actual sedimentation processes. Predicting centrifugal separation is as much based on heuristics involving properties like particulate sludge rheology, and particle resistance to shear degradation in the centrifuge feed zone (Bell, et. al., 1983). These uncertainties require scale-up to involve experiments at the pilot plant scale to predict large-scale behavior (personal communications, Rich Mathies, Alfa Laval). A test apparatus known as the Gyrotester has found use for predicting centrifugal behavior at large scales. The Gyrotester is a semicontinuous device (batch handling

of solids) that spins the suspension at set g-values making quantitation of the throughput and yield possible. This allows for a rational prediction of large-scale centrifugal performance for a given separation.

Because of these scale-up difficulties, equations 1 and 2 are useful for approximating the design parameters for centrifugal separation. Despite these limitations, the dependence of centrifugal separation on the square of the particle size and on the density difference between the particle and the mother liquor are reasonable assumptions. Obtaining a robust process that reproducibly produces particles of a separable size and density, and maintains an acceptable particle purity is the goal of the design engineer. The next sections will discuss how particle size, density, and purity are determined by the mechanism of particle formation.

Formation of Precipitates by Polyelectrolytes: The cationic polymer polyethyleneimine (PEI) was patented for use as a protein enrichment aid in 1972 (Boehringer Mannheim, 1972). PEI proved so effective it was incorporated into roughly one-third of the enzyme preparation procedures used at Boehringer Mannheim (Bell, et. al.,1983). PEI treatment aids in protein purification by increasing the separability of lysate debris. PEI

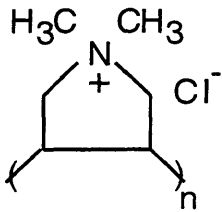
treatment increases particulate size by crosslinking debris. Additionally, PEI precipitates nucleic acid polymers, which are primarily responsible for the high viscosity of cellular lysate. Both effects improve liquid-solid separation by centrifugal means. Besides complexing debris and nucleic acids, protein-specific association occurs, which has been used for small-scale preparation of a number of enzymes, including RNA polymerase from *Escherichia coli* (Burgess and Jendrisak, 1975), RNA polymerase II from wheat germ (Jendrisak and Burgess, 1975), hexokinase from bakers yeast, and glucose oxidase from *Aspergillus niger* (Boehringer Mannheim, 1971).

A more diverse set of cationic polymers with varying charged properties have also been patented as protein purification aids (Eastman Kodak, 1977). Synthetic polyelectrolytes are easy to produce, making them inexpensive. Complexation occurs based on stoichiometric binding to anionic species, thus solutions can be diluted without the cost of additional precipitant. This is not the case for precipitation based on bulk solvent composition changes, e.g., ammonium sulfate precipitation. Facilitating polyelectrolyte precipitation was explored by introducing a polyaspartate tail to β -galactosidase (Parker, et. al., 1990). PEI precipitated the chimera protein along with nucleic acids and other anions. Problems in resolubilizing the

recombinant product were circumvented by adding a DNA digestion step prior to polymer precipitation. At larger scales this approach would be economically prohibitive. For the current project, the protein of interest (SELP) remains in solution during the polyelectrolyte treatment. This is due to the low number of anionic residues in the sequence of SELP available for binding to the cationic polymer. The polyelectrolyte treatment, then, fulfills the role of removing anionic impurities including proteins, nucleic acids and cellular debris, which otherwise present processing difficulties.

Precipitation by polyelectrolytes is based primarily on ionic interactions. Hence, variables that determine the performance of ion exchange chromatography, such as ionic strength and pH are similarly important for polyelectrolyte precipitation. The polymer can be titratable, as with PEI, or nontitratable, as with polymers containing quaternary amines. In this research, PEI is compared with the quaternary amine based polymer Poly(dimethyldiallylammonium chloride) (PDMDAAC) for their efficacy to assist removal of components of *Escherichia coli* lysate. This comparison is based on both impurity removal and separability of the precipitated material. Pertinent characteristics of these polymers are shown in Table II.

Table II: Cationic Polymer Characteristics

	<u>Polyethyleneimine</u>	<u>PDMDAAC</u>
Repeat unit	$\text{-(CH}_2\text{CH}_2\text{N)}_n$	
pKa	~10.5	N/A
Molecular mass	50,000/500,000	400,000

These polymers are expected to perform differently, much as a titratable ion exchange resin (weak exchanger) performs differently from a non-titratable resin (strong exchanger). PDMDAAC is positively charged over the entire pH range, and thus can be used at pHs where PEI is uncharged.

Published research on protein-PDMDAAC interactions is limited to physicochemical characterization of bovine serum albumen-PDMDAAC model systems (Dubin and Murrell, 1988). Precipitation of nucleic acids or cellular debris by PDMDAAC has not been reported, but polymers of similar charge properties have shown efficacy in precipitating cellular debris (Eastman Kodak, 1977). Hill and Zadow (1978) compared the ability of a polystyrene-based quaternary amine polymer to PEI for precipitating whey

proteins. At constant polymer concentration, the quaternary amine precipitated 95% of the whey protein, compared with 85% by PEI. Both polymers had an optimal pH near 10. Using a constant polymer concentration excluded the possibility that a greater polymer concentration is needed at higher pH. Polyelectrolytic complexation is predominantly by a mechanism of ionic interaction. More polymer is needed to neutralize the greater anionic content that is present at higher pHs. Additionally, PEI has an amine functionality with a pKa of 10-11. Thus, at high pH more polymer is needed due to the lower fractional ionization of PEI.

In summary, pH and polymer concentration for conducting a polyelectrolyte precipitation of bacterial lysate must be specified. It is expected that at higher pH, more polyelectrolyte will be needed for optimal impurity removal. Quantifying the removal of impurities and the separability of the solid is important to determine optimal conditions.

Formation of Precipitates by Salting-Out: The formation of a precipitating phase also occurs as a result of a change in solution characteristics (temperature or composition), which lowers the equilibrium solubility. Precipitation in response to changing the ionic

composition of the solution are classed as either salting-in or salting-out. With salting-in, protein solubility decreases with decreasing salt concentration due to increased dipole and induced dipole interactions between protein species (Scopes, 1994). Salting-out, in contrast, is the process where the protein solubility decreases with increasing salt concentration. The driving force for this behavior is hydrophobic interactions, i.e., minimizing the contact area of solvent-exposed hydrophobic patches. The effectiveness of a given salt for precipitating proteins is related to its location in the lyotropic series. This relationship is discussed in detail in the seminal work of Melander and Horvath (1977). Although many salts can be used, the focus here will be on salting out by ammonium sulfate, which has found the most widespread use. Ammonium sulfate is less expensive than other salts and the solutions have a lower density, which enhances the productivity of centrifugal recovery. Reviews of Scopes (1994), Rothstein (1993), and Foster (1994) provide a more complete treatment of precipitation processes in protein purification.

The solubility of proteins in salt solutions is expressed by the semi-empirical relationship attributed to Cohn (1925) as:

$$(3) \quad \text{Log}(S)=\beta-KI$$

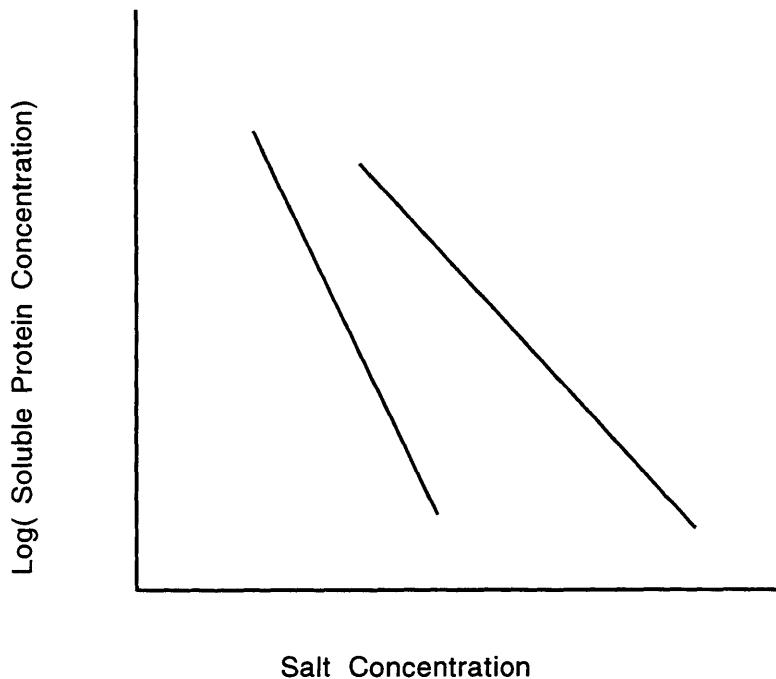
Where S is the soluble protein concentration, I is the ionic strength and β and K are constants. The constant K has been shown to be a function of the precipitant and the protein, whereas β depends on the protein, temperature, and pH. Solubility is usually at a minimum at the pH corresponding to the protein's isoelectric point (Bell, et. al., 1983). A rise in temperature commonly causes a decrease in β , presumably through an increased hydrophobic driving force, although the opposite behavior has been reported (Dixon, 1961).

Impurity Removal: Effect of Temperature, pH, and Dilution: In addition to the solubility of the target protein, the purity of the precipitate is also influenced by temperature, salt type and concentration, protein concentration, and pH. Temperature affects the solubility of protein impurities as well as the target protein. Slowly increasing the temperature at a given ammonium sulfate concentration has been suggested for obtaining well-ordered, and hence more pure crystals from ammonium sulfate solutions (Dixon, 1961). Impurities have a lower solubility at their isoelectric point, thus operating away from this pH will produce a purer precipitate. Ideally, one should operate near the target protein's isoelectric point but away from the isoelectric point of impurities to

optimize purity and yield. Experiments utilizing an assay for impurities, as well as the target protein are needed to determine optimal conditions for the purification operation.

The effect of protein concentration on impurity removal is illustrated by referring to the hypothetical solubility curves for two proteins shown in Figure V, where the curves on the left and right illustrate the solubility behavior of the protein of interest and an impurity, respectively. By starting the precipitation from a more dilute solution, one can dilute the impurity to a point where it remains soluble, while the protein of interest precipitates. This dilution effect occurs when the K_s for the protein of interest is larger (steeper slope) than the impurity. When the K_s for the impurity is larger than the protein of interest, diluting the solution will result in a more impure product.

Figure V: Precipitation Behavior of Two Hypothetical Proteins



Economic factors can become important when determining the appropriate dilution to conduct the precipitation process. For a more dilute solution, more salt is needed, both because of the larger volume of solution, and because a higher salt concentration is needed to give the same yield. This results in higher reagent and waste disposal costs, longer processing times, and larger precipitation reactors. In processes where precipitation is a critical purification step, multiple precipitations may be necessary. Determining the optimal protein concentrations for each precipitation step incorporates economical and technical considerations and represents a

significant design optimization challenge.

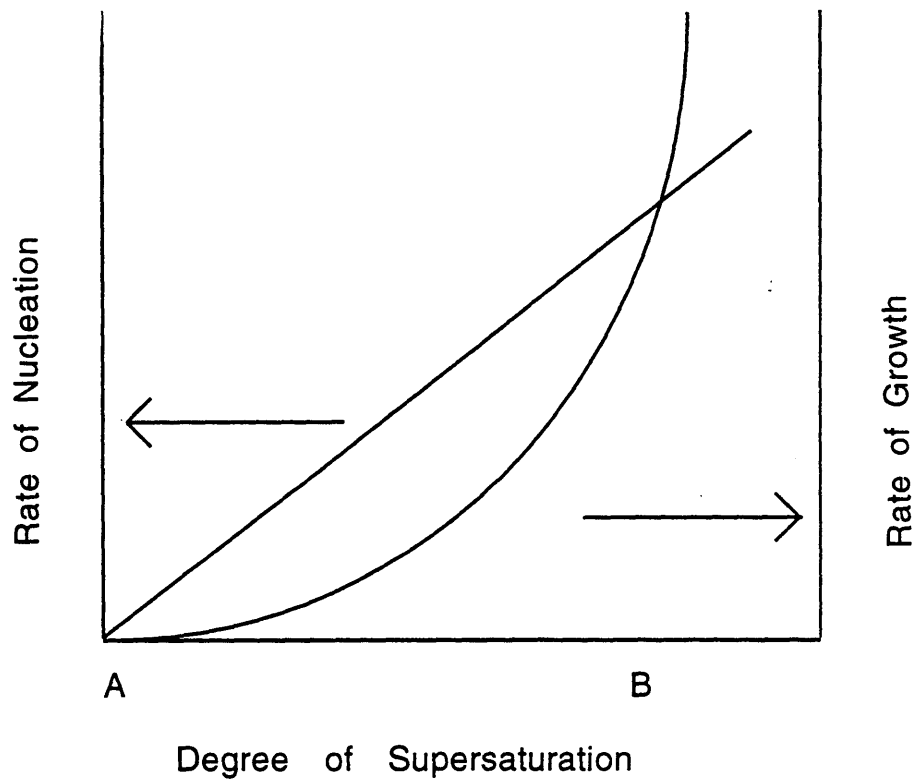
Kinetic Factors Affecting the Separability of Particulates: In contrast to the equilibrium behavior of precipitation phenomena for small molecules, the precipitation behavior of proteins is potentially nonreversible and determined by competing kinetic processes. Thus the apparent protein solubility is determined in part by factors such as precipitant concentration, addition and mixing rates, and type of contacting vessel. Illustrating this effect is the behavior of fumarase (Foster, 1976). Depending on the method of contact (tubular reactor vs. batch or continuous stirred tank reactor) and the concentration of ammonium sulfate added (solid vs. saturated liquid) the amount of salt required to obtain the same yield varies from 55% saturation (batch reactor, solid ammonium sulfate addition) to 75% saturation (continuous stirred tank reactor, saturated ammonium sulfate solution addition).

In addition to apparent solubility, the size, density, and purity of the particulates are also affected by the process of particle formation. This process can be divided into three steps: nucleation, growth, and aging.

Nucleation is the formation of primary particles in response to a change in

the solution (composition, temperature, pH) that energetically favors a particulate phase. The formation of nuclei occurs under supersaturated conditions. The higher the degree of supersaturation, the faster the kinetics of nucleation. Once particles are present, a kinetic competition occurs between growth of existing particles and nucleation of new particles. This behavior is shown in Figure VI (Rothstein, 1993). At higher degrees of supersaturation, nucleation processes dominate, resulting in a large number of small particles. Since larger particles are easier to separate, it is advisable to operate in a regime where growth occurs at an acceptable rate and the rate of formation of new nuclei is kept low. Particle growth occurs via two mechanisms. Diffusion-limited adsorption of proteins and primary particles (perikinetic growth) and convection-induced collisions of primary particles and aggregates (orthokinetic growth). The final aggregate size increases by these mechanisms until either all interparticle binding sites are occupied, or until shear-induced breakup of larger particles becomes dominant. The balance between interparticle adhesive forces, and shear-induced breakage determines the final distribution of particle sizes in solution.

Figure VI: Kinetic Competition between Particle Nucleation and Growth



Aging of particle can improve both purity and separability. During aging, the suspension is submitted to a controlled mixing environment, where reshuffling of molecular structure occurs in response to intraparticle vibrations. This reshuffling produces a denser and potentially more pure particle as impurities due to overprecipitation and entrainment have a chance to redissolve. Industrial centrifuges characteristically have a zone of high shear at the feed port, where the mixture is accelerated to the

velocity of the centrifuge. This high shear environment can breakup particles, resulting in poor separations. This effect can be partially offset by using centrifuges designed to accelerate the feed in a low shear manner, such as that suggested for separation of shear-sensitive hybridoma cells (Tebbe, et. al., 1996). Alternatively, aging processes potentially strengthens particles which reduces their shear sensitivity and thus decreases breakup during centrifugal separation. This has been found to be essential for the robust operation of some currently used precipitation operations (Rothstein,1993).

The important variable determining the extent of aging is the Camp number, a dimensionless product of the aging time and the root mean square velocity gradient in the vessel, which is related to the power per unit volume (Bell, et. al., 1983). Camp numbers up to 10^5 have been shown to improve particle strength, as measured by resistance to shear breakup, of soy bean precipitates formed by isoelectric precipitation (Bell, and Dunnill, 1982). Aging also strengthens precipitates prepared from casein (Hoare, 1982) and human serum (Foster, et. al., 1986). The aging process can be accelerated by acoustic conditioning, which uses ultrasonic generators to increase intraparticle vibrations (Bell and Dunnill, 1983). A continuous

process for the fractionation of human serum, based on the Cohn process (Foster, 1986) utilizes a continuous tubular reactor to generate particles. An early protocol used acoustic conditioning prior to centrifugal recovery, but this has since been replaced with a simpler conditioning device based on a special static mixer designed to minimize problems associated with adherence of sticky proteins.

There are two extreme particle characteristics that create problems in centrifugation operations: fragile particles and sticky particles. Fragile particles are shear-sensitive and breakup in the high shear zone of continuous centrifuges, making their recovery problematic. At the other end of the spectrum, particles composed of extremely sticky proteins generally aggregate to a single particle if given the chance, and will stick to surfaces. Losses due to nonspecific adsorption to surfaces can potentially be very high. A strategy of producing the particles in near vicinity to centrifugal recovery, for instance in a continuous tubular plug flow reactor, is one way of circumventing this problem. A design for a static mixer for the continuous aging of the sticky precipitates associated with serum protein fractionation is discussed in McIntosh, et. al. (1989). For sticky proteins, manual collection of solids is required due to problems

with plugging of the continuous discharge port of the centrifuge.

Precipitation Reactor Designs: The reactor configuration can significantly impact both recoverability and purity of particulates. In a study of the recovery of soya protein precipitates formed by acid addition to the isoelectric point, significant differences in the particle resistance to shear, as measured by scroll discharge centrifuge performance, was observed between particles formed in a tubular reactor, and those formed in a stirred batch reactor (Bell, et. al. ,1982). The batch reactor produced particles that were more shear-resistant and regular in size than the tubular reactor. In the previously reported ammonium sulfate precipitation of fumarase (Foster, et. al., 1976), the reactor configuration (batch or continuous stirred tank reactor), as well as the state of the ammonium sulfate (solid vs. saturated liquid) dramatically affected the apparent solubility constant, with batch precipitation occurred at up to 25% less of saturation than precipitation in a continuous stirred tank configuration. Nelson and Glatz (1985) showed that primary particles formed from soy proteins in a batch reactor were smaller than those formed in a CSTR (continuous stirred tank reactor), and suggests as the reason that CSTR-produced primary particles are formed from a more dilute solution, and

hence fewer nuclei were formed.

The effect of reactor configuration on particulate purity is expected to be due primarily to mixing effects. Tubular reactors, as a result of very fast mixing compared to batch reactors, minimize the overprecipitation of impurities. This is most prevalent at larger scales due to inefficiencies of scaling-up batch mixing. Tubular reactors minimize vessel size and allow for continuous processing, providing significant economic advantages over batch processing. A continuous process in operation for the cold ethanol fractionation of serum proteins is described by Watt and Smith (1971) and Foster, et. al. (1986) as having significant advantages over the batch process, with the main obstacle to widespread acceptance being the close tolerances of pH and temperature that are necessary for robust operation. Despite the benefits of tubular reactors, current industrial precipitation processes are dominated by batch reactors. The precipitating reagents are introduced by either spraying across the surface or by sparging near the zone of maximal dispersion of the mixers (Foster, 1994). The reason for this is unclear, but perhaps continuous processes are more suitable for processes where kinetic nuances that control the outcome are less important. Alternatively, variability in the feed (as a result of batch

derived feedstocks) may make determining parameters for continuous operation difficult. Additionally, design engineers may allow historic precedent to dictate new process design. Advances in on-line control which allow for real-time analysis of separation efficiency may enhance the ability to control continuous precipitation processes. One such instrument, consisting of a high speed microcentrifuge in conjunction with a flow injection analyzer, can analyze solubility data in about 200 seconds (Niktari, et. al., 1990).

In summary, the performance of precipitation operations for protein purification is dependent on a number of variables. Developing an effective process involves determining operating parameters which maximize particulate recovery and minimize impurity carryover. Thus, the effect that pH, temperature, and protein concentration have on particulate purity and solubility should be elucidated. This can be done best if there are robust assays for both the protein of interest and pertinent impurities. The potentially kinetic and irreversible nature of the phenomena illustrates the importance of carrying out experiments at progressively larger scales to design a process for large-scale production. Although currently not the norm, continuous processes have many advantages over batch processes,

both economically, by reducing process volumes, and technically, by reducing zones of overprecipitation. The application of continuous processes is dependent on the ability to tightly control operating parameters to produce separable particles.

IV. MATERIALS AND METHODS

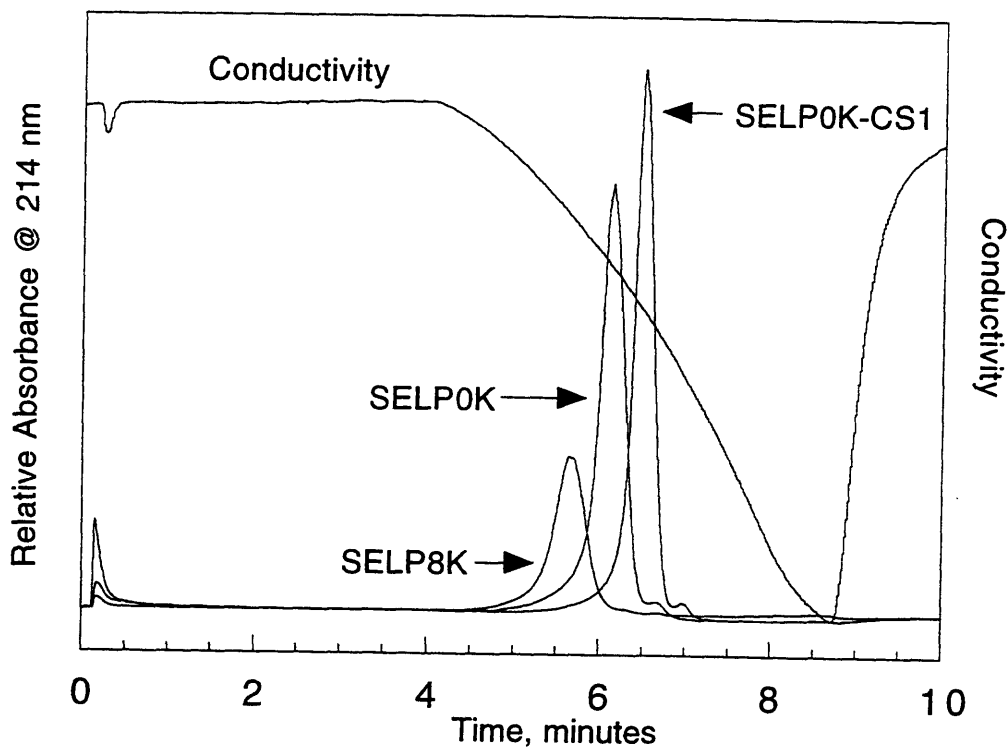
SELP standards and *Escherichia coli* lysate containing SELP, were supplied by Protein Polymer Technologies, Inc. (San Diego, CA). The lysate was prepared at Protein Polymer Technologies, Inc., as follows: Three kilograms of frozen cells were thawed and resuspended in 12 liters of water. Three passes through a high pressure homogenizer (Manton-Gaulin) operating at 8000 psi were used to disrupt the cells. This material was shipped frozen as 40 ml aliquots, which were thawed at room temperature on the day of a given experiment. During the course of this research, three different SELP species were used: SELP8K, SELP0K, and SELP0K-CS1. The differences between these species is described in chapter I. Lot numbers for the various SELP species used as standards in this work are: SELP8K- 95086 and 95091; SELP0K- 95121; SELP0K-CS1- 95711. Lot numbers for *Escherichia coli* lysate containing the various SELP species used in this work are: SELP8K- 95113, SELP0K- NB183/24, SELP0K-CS1- 96021. Water for all experiments was produced by a MilliQ water purification system (Millipore, Bedford, MA).

Assay Development: An HPLC assay was developed to facilitate the calculation of SELP yield in each purification step. Many different chemistries were screened for the ability to selectively bind SELP including immunoaffinity, metal chelate, ion exchange, and hydrophobic interaction chromatography. These attempts resulted in extensive characterization of SELP, which is reported later. Hydrophobic interaction chromatography (HIC) is the technique which proved useful as an assay and is described here.

POROS™ HIC media (Perseptive Biosystems, Framingham, MA) was used for all assay development and analytical runs. Analysis was performed on a BioCad™ HPLC system (Perseptive Biosystems, Framingham, MA), with the UV detector set at 214 nm for monitoring peaks. Columns of dimension 2.1 mm X 30 mm were self-packed, using a column packer obtained from Perseptive Biosystems with a custom adapter designed to allow packing of small columns. The flowrate for all runs was 5 ml/minute, giving a superficial fluid velocity of 8600 cm/hr. Chromatograms, including reequilibration of the column, were obtained in approximately 10 minutes. Binding of SELP to the HIC media was accomplished by injecting a sample containing SELP onto a column equilibrated with an ammonium sulfate

(Mallinckrodt, Paris, KY) loading solution. To elute, a gradient or step change to a lower ammonium sulfate concentration was used. Both the elution and binding solutions were buffered at pH 5.5 with 0.25 g/L of the Goods buffer morpholino ethane sulfonate (MES) (SIGMA, St. Louis, MO). Figure VII shows chromatograms of different SELP species on the POROS PE™ media.

Figure VII: Hydrophobic Interaction Chromatography Behavior of Different SELP Species



Two additional hydrophobic interaction media, Poros PH™ and HP™, were

also found to selectively bind SELP. The actual conditions for SELP elution depends on the type of HIC media, and the SELP species, which is shown in Table II. These conditions are determined from chromatograms such as those in Figure VII, and reported as the ammonium sulfate concentration (calculated from the online conductivity detector output as shown in Figure III) at the apex of the elution peak using a shallow elution gradient of 100. g/L to 0. g/L ammonium sulfate over 200 column volumes.

Table III: Concentration of Ammonium Sulfate at the Apex of the SELP Elution Peak

<u>HIC Media</u>	<u>SELP8K</u>	<u>SELP0K</u>	<u>SELP0K-CS1</u>
POROS TM PE	78.1 g/L AS*	70.3 g/L AS	62.1 g/L AS
POROS TM PH	74.2 g/L AS	68.3 g/L AS	not determined
POROS TM HP	~45 g/L AS	~20 % AC**	not determined

* AS=Ammonium Sulfate, .25 M MES, pH 5.5

** AC= Acetonitrile

The hydrophobicity of the column packing increases from PE to PH to HP. Inspection of the concentration of ammonium sulfate at the apex of the elution peak for the various SELP species indicates an order of increasing

hydrophobicity of SELP8K, SELP0K, and SELP0K-CS1. The POROS HP media actually binds SELP0K (and probably SELP0K-CS1) in a “reversed phase” mode, with approximately 20% acetonitrile used for elution. The ability of the POROS HP media to selectively bind SELP0K directly from lysate is of potential use as a large-scale purification method. Based on the HIC assay, the concentration of SELP in the supplied lysate was determined to be 4.1 g/L, 4.6 g/L and 4.9 g/L for SELP8K, SELP0K, and SELP0K-CS1 respectively.

Immobilized Metal Affinity Chromatography (IMAC): Experiments were performed with a POROS™ 20 MC self-packed column (4.6 mmD X50 mL) (Perseptive Biosystems, Framingham, MA). The solid support uses immobilized iminodiacetate (IDA) functionalities to coordinate metal binding. Metal salt solutions were loaded as per instructions. Nickel chloride was found to performed marginally better then copper sulfate (results not shown). The loading buffer was 20 mM phosphate, 0.5 M NaCl, pH 7.0 or higher, as well as one case at 0.01 M NaOH, pH 12. Elution was accomplished with 20 mM to 200 mM NaH₂PO₄, 0.5 M NaCl, adjusted to pH 4.5. Peak monitoring was at 214 nm, thus the more typical imidazole elution was avoided due to the high absorbance at 214 nm of imidazole solutions.

Cation Exchange Chromatography: Experiments were performed with a POROS™ 20 HS self-packed column (4.6 mmD X 50 mmL) (Perseptive Biosystems, Framingham, MA). Buffer conditions for binding were either 0.005 M or 0.01 M MES pH 5.5 for loading, and the same with 1M NaCl for elution. Protein solutions were dissolved in pH 5.5 MES for approximately 30 minutes and filtered (< 0.22 µM) just prior to analysis. These solutions were stable, as judged by repeated runs, for several hours. A 20 column volume gradient to 1M NaCl was used for collecting fractions. Manually collected fractions were diluted 3 fold in running buffer and reanalyzed. Collected fraction were also analyzed for amino acid content at Protein Polymer Technologies (PPT). In addition cyanogen bromide treated SELP8K, obtained from PPT, was also analyzed by cation exchange chromatography at the conditions listed above.

Size Exclusion Chromatography (SEC): Runs were performed with a Beckman ultraspherogel SEC 3000 column (Beckman Instruments, Fullerton, CA) with an attached guard column. The buffer conditions were 20 mM Phosphate, pH 7.5, 150 mM NaCl. A flowrate of 0.5 ml/min was used for all analysis, with an injection volume of 10 µL. Proteins of known molecular weight were used off the shelf as standards. The bovine serum albumen

solution contained sodium azide, which served as a marker to determine the total accessible column volume. Blue dextran was used to determine the void volume.

Polyelectrolyte Precipitation: Polyethyleneimine of 50,000 MW (SIGMA, St. Louis, MO) and 500,000 MW (Aldrich, Milwaukee, WI) were obtained as a 50 wt/vol% solution. The quaternary amine-based polymer, Poly(dimethyldiallyl ammonium chloride) (PDMDAAC), was supplied as a 50 wt/vol% solution by Calgon Corp (Pittsburgh, PA), under the trade name Merquat 100. Stock polymer solutions were made by weighing out 5 grams of the highly viscous 50 wt/vol% solution and making up to 50 ml with water, resulting in a 4.8 wt/vol% solution. This solution was adjusted to the pH of the experiment with concentrated hydrochloric acid (Mallinckrodt, Paris, KY). Aliquots of this stock solution were further diluted for each experiment such that the desired concentration of polymer was obtained when mixed with an equal volume of lysate. The 4.8 wt/vol% PEI stock solution was stored at 40C and was not used if older than one week, as precipitates became apparent upon storage for longer times. Polymer solutions were adjusted to a specific pH on the day of the experiment to avoid minor pH changes which occur as a result of long-term exposure to

airborne CO₂. For experiments determining the effect of pH on polymer precipitation, SELP-containing solutions were adjusted to the pH of the experiment with 5M NaOH (Mallinckrodt, Paris, KY), taking care to add the concentrated base at the zone of high mixing to minimize any effects from localized high pH.

The mixing rate and polymer addition rate are important variables in the outcome of precipitation reactions. To minimize experimental variations due to mixing and polymer addition, care was taken to perform the polymer addition in an equivalent manner for all experiments. Mixing the polymer and lysate together was accomplished by rapidly adding the polymer solution to the lysate and quickly vortex mixing in 1.7 ml polypropylene microcentrifuge tubes (VWR). After thorough mixing, the solutions were allowed to settle for 15 minutes and a visual determination of the extent of settling was obtained. The solutions were then centrifuged at 10,000 rpm for 10 minutes in a refrigerated microcentrifuge (Baxter Scientific). The resulting supernatants were sampled and assayed for SELP by the forementioned HIC assay, and for impurity proteins by the Coomassie Blue protein assay (Bradford, 1976) (Biorad, Richmond, CA). SELP proteins do not produce a significant response to the Coomassie Blue protein assay,

presumably because the Coomassie dye response is specific for proteins with a high aromatic and cationic amino acid content (Tal, et.al., 1980). Thus, the Coomassie Blue assay was utilized to comparatively judge the effect of pH and polymer concentration on the removal of protein impurities. Bovine serum albumin (2.0 mg/ml ampules, PIERCE, St. Louis, MO) was used as the protein standard for all protein analysis. Both PEI and PDMDAAC were found to interfere with total protein assays based on cupric ion reduction such as the Lowry assay and BCA assay (PIERCE, St. Louis, MO). A modified Lowry assay (Biorad, Richmond, CA) was used to determine the concentration of SELP solutions used as HPLC standards.

PEI-lysate suspensions for hindered settling tests were prepared by mixing 12.5 ml of lysate with 12.5 ml of 0.8 wt% PEI, both at pH 8 and room temperature. The polymer and lysate were contacted under two different mixing regimes, designed to bracket conditions expected at larger scales. A fast-addition, slow-mixing case was performed by quickly adding the polymer solution to a slowly stirred lysate solution (approximately 1 revolution every 2 seconds); overall mixing time was estimated by the appearance of a uniform consistency to be approximately 30 seconds. A slow-addition, fast-mixing case was performed by stirring lysate at a rate

to ensure good vortex formation, and adding the PEI solution dropwise, allowing the solution to become well mixed after each drop. The overall PEI addition time was in excess of 2 minutes. The resulting solutions were transferred to 25 ml graduated cylinders and the height of the interface between clear liquid and the suspension monitored as a function of time.

Ammonium Sulfate Precipitation: Ammonium sulfate precipitation experiments were conducted on the supernatant of the PEI precipitation step, prepared as follows: 40 ml of 0.8 wt% polyethyleneimine was added to 40 ml of lysate, both at pH 8 and room temperature, stirred for 10 minutes, centrifuged at 3,500 g for 10 minutes (Beckman(Palo Alto, CA) model TJ-6R, TA-10 rotor). The supernatant was decanted and used for characterizing the precipitation of SELP by ammonium sulfate. Analysis of the supernatant by the Coomassie Blue total protein assay and the HIC assay for SELP showed insignificant batch-to-batch variations.

Saturated ammonium sulfate was prepared by adding 530 grams of solid ammonium sulfate (Mallinckrodt, Paris, KY) to enough water to make a final volume of 1 liter. The solution was stirred for at least 2 hours, filtered through a 0.2 μ m membrane, and enough ammonium sulfate was added to

maintain some solid in the reagent bottle, thus insuring saturated conditions. No correction for temperature was made, as the solubility of ammonium sulfate in water is only weakly dependent on temperature (Scopes, 1994)

The solubility of SELP in ammonium sulfate solutions was determined with both prepurified SELP and with the supernatant from the PEI precipitation step described above. For the prepurified SELP, solutions of specific ammonium sulfate concentrations spanning the range of interest were made up, and SELP was added from a stock solution with rapid mixing. A tenfold dilution of SELP occurred during this process. These solutions were allowed to equilibrate for at least two hours, centrifuged for 20 minutes at 10,000 rpm in a microcentrifuge, and assayed for total protein by a modified Lowry assay (Biorad, Richmond, CA). For the precipitation of SELP from the PEI-treated lysate supernatant, the SELP-containing solution was stirred while adding the saturated ammonium sulfate dropwise. As with the polymer precipitation experiments, care was taken to ensure that a similar stirring and reagent addition protocol was used for each experiment. Solubility data of SELP from the polymer treated lysate supernatant was obtained by slowly adding saturated ammonium

sulfate to the SELP-containing solution. The cumulative volume of ammonium sulfate added at the point of cloudiness was recorded. Additional aliquots of ammonium sulfate were added dropwise, and samples taken. By careful accounting of the sample volume and the volume of ammonium sulfate added, the ammonium sulfate concentration in each sample was calculated. The samples were spun in a microcentrifuge at 10,000 rpm for 20 minutes, and the supernatants analyzed for SELP by the forementioned HPLC assay. Solubility data at 4°C were obtained in the same manner as above, with everything located in a 4°C coldroom. SELP and saturated ammonium sulfate solutions were equilibrated beforehand at the temperature of the experiment.

Microscopic examination and photographic characterization of precipitates formed under different conditions of mixing, reagent addition, and aging were performed on a microscope equipped with phase contrast lenses and a 35mm SLR camera system (Nikon OptiPhot, DSC Optical Services, Natick, MA). Solutions were placed on microscope slides with concave indentations, and a coverslip placed on top. Visual inspection showed no evidence of further aggregation after the slides were prepared.

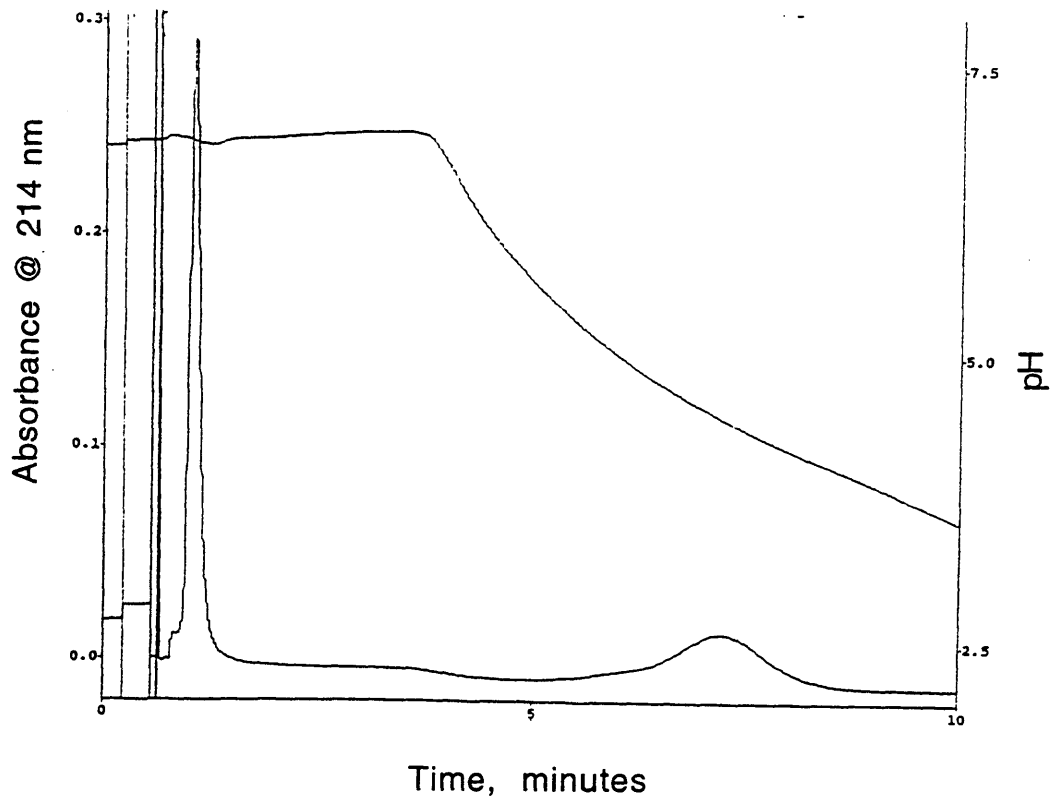
Samples sent to Protein Polymer Technologies, Inc. for additional analysis were further processed by dialysis against either 3500, or 10,000 MW cutoff dialysis tubing (Spectrum Medical Industries Inc., Houston, TX). Samples containing approximately 20 mg/ml SELP were dialyzed for greater than eight hours against two one liter changes of water. These samples were split into four milliliter aliquots and lyophilized for greater than 24 hours.

V. RESULTS and DISCUSSION

Characterization of SELP8K: During the course of developing a HPLC based assay for SELP, a body of knowledge was developed on solution characteristics of SELP8K. Whether these results are more broadly applicable to other SELP species is unknown. The results of these characterizations are presented here to assist in explaining phenomena that may be encountered with SELP, and to guide in the development of laboratory techniques to characterize further the solution behavior of SELP.

Immobilized Metal Ions Chromatography (IMAC): The best observed conditions for binding, shown in Figure VIII below, resulted in approximately 40% of SELP8K adsorbing to the column. For this highest binding case, protein was dissolved in pH 5.5 morpholino ethane sulfonate (MES) at 0.02 M, and diluted into a phosphate pH 7.5 buffer prior to analysis. Other runs resulted in significantly less adsorption, and reproducibility of results was the exception, rather than the rule. The pH gradient on the chromatogram shown in Figure VIII is offset from the actual gradient observed.

Figure VIII: Immobilized Metal Affinity Chromatography of SELP8K



Elution occurs at a pH of between 6.5 and 5.5 due to the protonation of the histidines. In general, column performance deteriorated quickly, with only a few runs being possible before unstable results are generated, requiring column regeneration. This is probably due to either stripping of the metal from the IDA sites on the packing at low pH or metal transfer to the protein. Both mechanisms have been observed in other systems (Sulkowski, 1985, Porath, 1992).

Cation Exchange Chromatography: As shown in Figure IX, at the conditions used (0.01 M MES, pH 5.5), SELP8K is separated into three different ionic species, a low salt eluting species (46% total area), a middle salt eluting species (11% total area), and a high salt eluting species (43% total area). Also shown in Figure IX are chromatograms of collected fractions that were reinjected which confirms that these are separate species, and not an equilibrium distribution of conformations. An attempt to analyze these fractions by metal chelation proved inconclusive. The results of amino acid analysis on collected fractions (reported in a PPTI internal document) reveal that material in peak one probably lacks amino acids from the C-terminus, including the polyhistidine tail. The second elution peak probably represents material deficient in amino acids from the N-terminus, and the third elution peak is probably full length SELP8K. This conclusion was tested further by analyzing cyanogen bromide treated SELP8K with cation exchange chromatography. Cyanogen bromide cleaves proteins at methionine residues, thus isolating the structural SELP protein from the flanking sequences (Figure I in Chapter I). As shown in Figure X, cyanogen bromide treated material elutes in a single peak at a low salt concentration, with a minor peak at higher salt concentration that probably represents unreacted SELP8K.

Figure IX: Cation Exchange Chromatography of SELP8K and Results from the Reinjection of Collected Peaks.

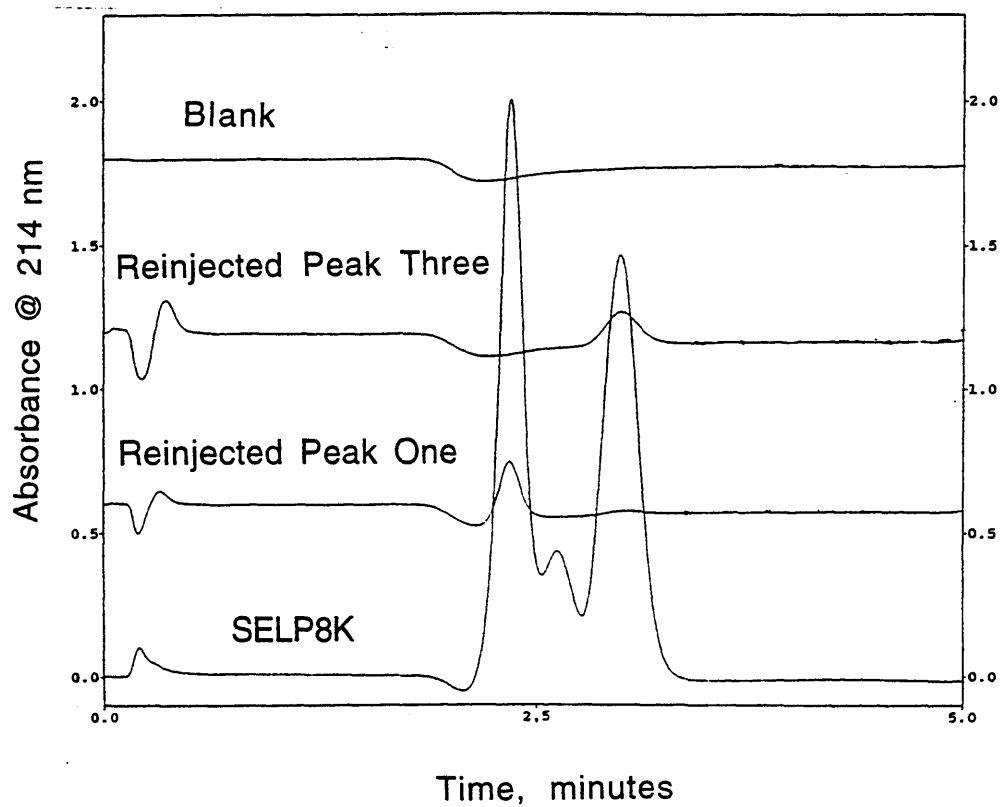
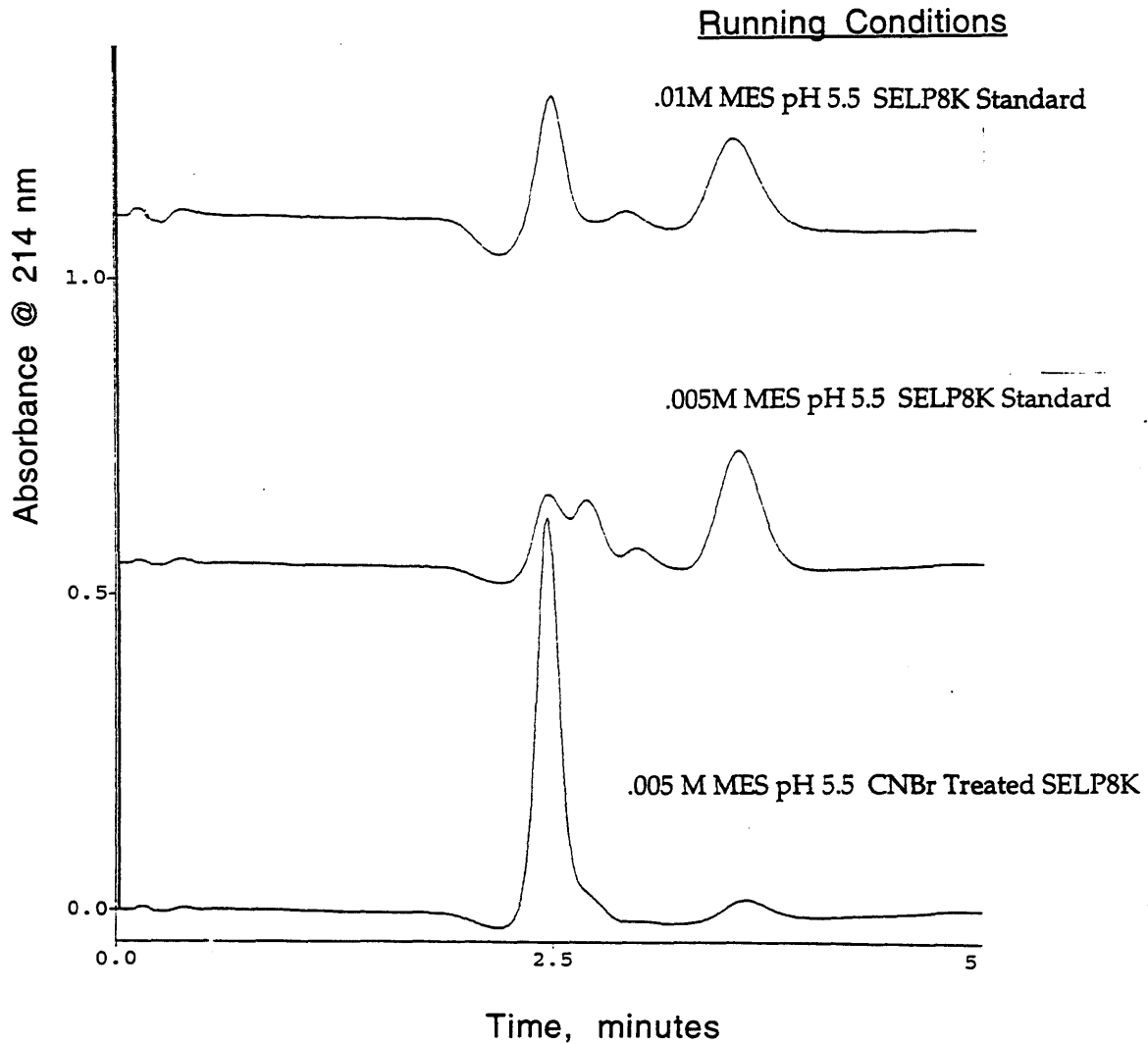


Figure X: Cation Exchange Chromatography of Cyanogen Bromide Treated SELP8K.



These results indicate that the ionic heterogeneity of SELP8K is due to differences in the content of amino acids associated with the leading and tailing sequences. The middle chromatogram of Figure X shows an additional

elution peak compared to the chromatograms of Figure IX, and the top chromatogram of Figure X. This extra elution peak is due to the weaker ionic strength of the binding solution, which allows a resolution of the material represented by peak one of Figure IX into two separate species.

Size Exclusion Chromatography: Figure XI shows the size exclusion chromatogram of SELP8K compared to other proteins of known molecular weight. The column calibration is shown in the insert graph. At the conditions used, SELP8K began eluting at a retention time characteristic of a globular protein with a molecular weight in excess of 200,000. The elution peak is broad and asymmetrical, which suggests a distribution of many species in solution. Figure XII shows SEC profiles for SELP8K at two different protein concentration, 0.35 and 3.5 mg/ml. At the higher protein concentration, a sharper peak at a retention volume of a higher molecular weight is observed. This is consistent with a concentration dependant association phenomenon. Interestingly, there also appears to be an upper limit to the size of the associated species, as indicated by the sharp forward edge of the SELP peak. This peak does not correspond to the void of the column, as measured by blue dextran.

Figure XI: Size Exclusion Chromatography Behavior of SELP8K

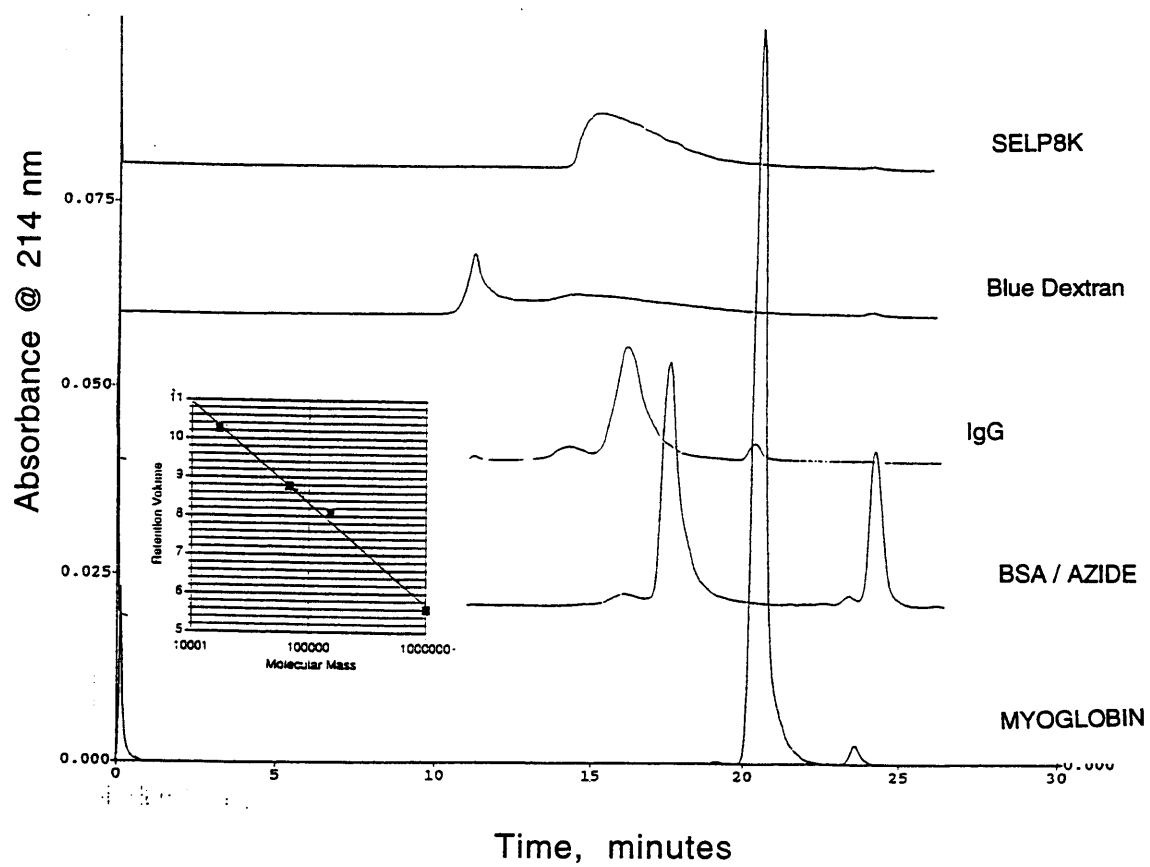
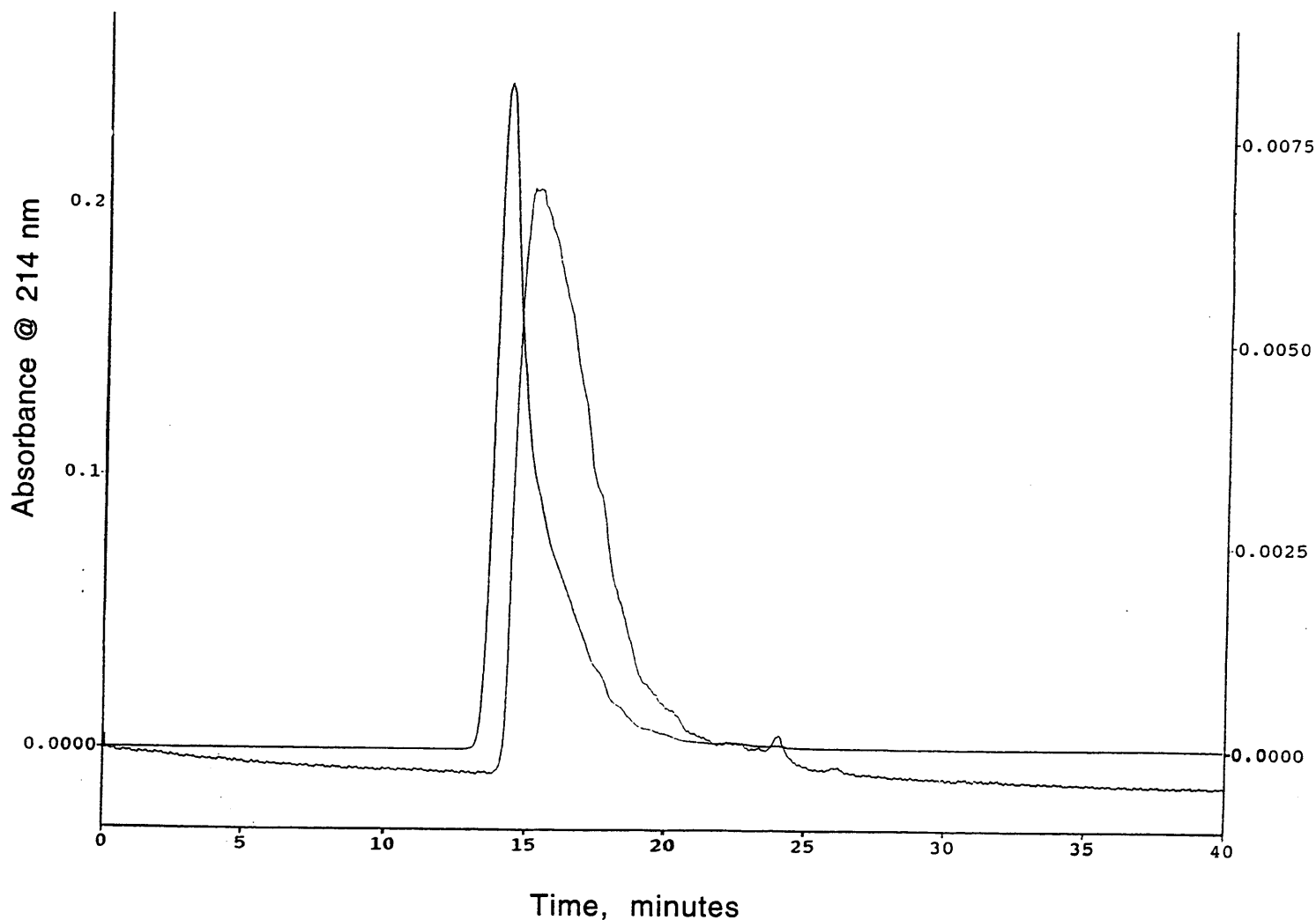


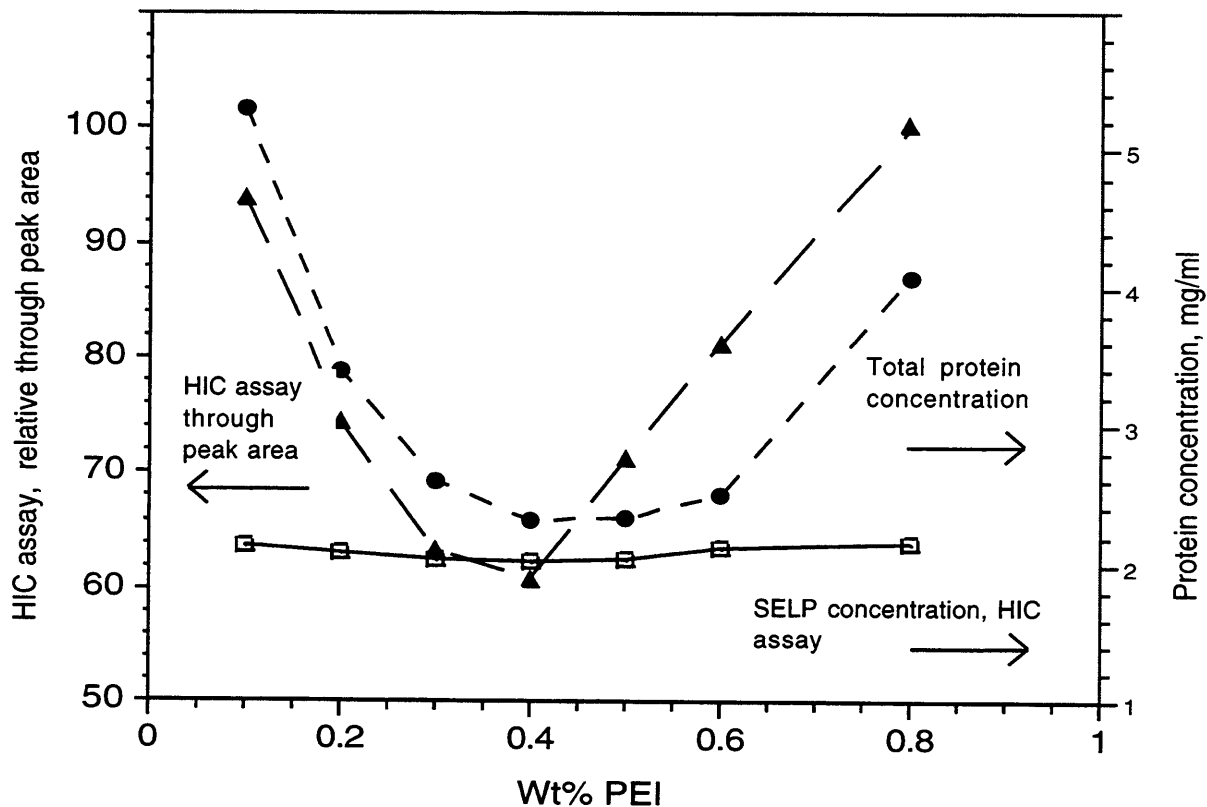
Figure XII: Effect of Protein Concentration on the Size Exclusion Chromatography Behavior of SELP8K



Polyethyleneimine (PEI) Precipitation: Mixing PEI with bacterial lysate produces a solid-liquid suspension which is easily separated to produce a liquid which is reduced in anionic species. Figure XIII shows the result of mixing SELP containing lysate derived from *Escherichia coli* with solutions containing PEI at various concentrations.

Figure XIII: Analysis of PEI Treated Lysate Supernatant, pH 7: Determination of Optimal PEI Loading for Lysate Flocculation.

● -Coomassie total protein assay. ▲ -HIC assay through peak area, relative units. □ -SELP concentration, from HIC assay.



The abscissa is the PEI concentration after mixing and the different ordinates are results from analysis of the supernatant obtained after centrifuging the suspension. Both the total protein concentration, as assayed by Coomassie Blue, and the HIC through-peak values show an optimal polymer concentration for the removal of impurities at about 0.4

wt% PEI. At this condition, approximately 2.2 mg/ml of impurity protein are present. This compares with 8 mg/ml in the untreated lysate. Thus an approximate fourfold purification is obtained at the optimal condition. The Coomassie Blue assay detects those proteins that bind to the Coomassie Blue dye (proteins rich in aromatic and basic amino acids exhibit tight binding and produce a strong response to the Coomassie Blue dye), whereas the through-peak area of the HIC assay correlates to molecules that absorb UV light at a wavelength of 214 nm, and represents a broader class of compounds. The corroboration of the two results suggests that a true optimum has been determined. Figure XIII also shows that at most 5% SELP is lost during the process. This loss may represent an artifact of the chromatographic assay, as the hydrophobic interaction column may be binding some host cell proteins which could be reported as SELP. Western blot analysis of the precipitate produced at the optimal PEI loading (not shown) indicate minimal or no SELP is present in the precipitate. The high observed yield of SELP (>95%) through the precipitation operation is consistent with the presence of only four anionic amino acids in the entire sequence (shown in Figure I) available for binding to the polymer. Additional evidence that the optimal conditions have been determined is provided by the observations that solutions nearer the optimal conditions

have a paler yellow color (less color) and require less pressure to filter through a 0.2 μm syringe filter.

The pH of the PEI precipitation process has a strong effect on impurity removal, as shown in Figure XIV. At every pH except at pH 10, an optimal PEI concentration is observed for the removal of impurities. At pH 10, PEI is largely uncharged and thus not as effective in binding anionic impurities. The optimal PEI concentration increases with pH, from 0.3 wt% at pH 6.5 to 0.7 wt% at pH 9. The level of impurity removal at the optimal conditions (determined at the lowest value of the Coomassie total protein results) also increases with pH, up to pH 10. At a pH of 6.5, 2.8 mg/ml protein is observed at the optimal condition of 0.3 wt% PEI, whereas at the optimal conditions at pH 8 and 9, 2.2 mg/ml of protein is retained. Since the original untreated lysate (diluted twofold for comparative purposes) contains approximately 8 mg/ml total protein, operating at pH 8 or 9 results in 21% greater impurity removal than at pH 6.5, and 8% greater than at pH 7.

Figure XIV: Effect of pH and PEI Concentration on the Removal of Protein Impurities from *Escherichia Coli* Derived Lysate.

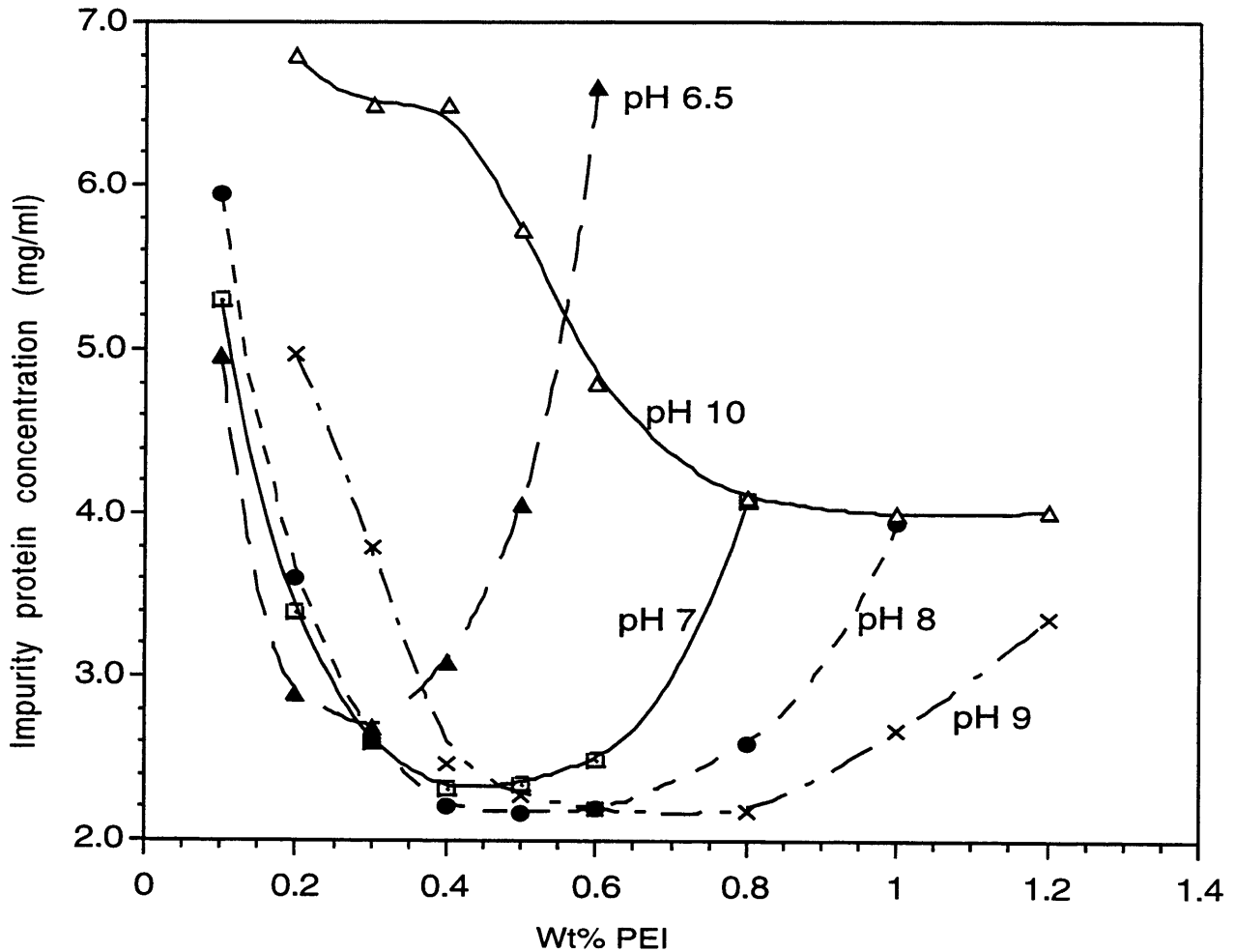


Figure XIV also shows that at higher pH's, a broader optimum is observed, which has important ramifications for process control. Performing the flocculation at a higher pH will result in a more robust process since slight deviations in feedstock composition or operating conditions will have less of an impact on impurity removal.

These results provide mechanistic implications on impurity removal by cationic polymers which will be discussed later. Results from the flocculation of lysate with a quaternary amine polymer will now be presented.

Poly(dimethyldiallylammonium chloride) (PDMDAAC) Precipitation:

The results on the removal of protein impurities from the SELP-containing lysate by the quaternary amine-based polymer PDMDAAC are shown in Figure XV. Similar to results presented for PEI, there exists an optimal polymer concentration for the removal of protein impurities at each pH tested. In contrast to PEI, operating at a pH greater than 10 results in significant improvement in impurity removal. For example, at a pH of 11.8, only 0.4 mg/ml of protein, as measured by the Coomassie total protein assay, remain in the supernatant. This compares with 2.0 mg/ml at pH 9.2, and 2.2 mg/ml in the best case for the PEI precipitation (Figure VIII, pH 8 or 9). Figure XV also shows that the amount of PDMDAAC necessary for optimal impurity removal does not appreciably change from pH 7 to 9.2 (0.3 wt%), whereas at pH 11.8, nearly twice the amount of polymer (0.5-0.6 wt%) is needed to achieve the optimal impurity removal.

FIGURE XV: Effect of pH and PDMDAAC Concentration on the Removal of Protein Impurities from *Escherichia Coli* Derived Lysate.

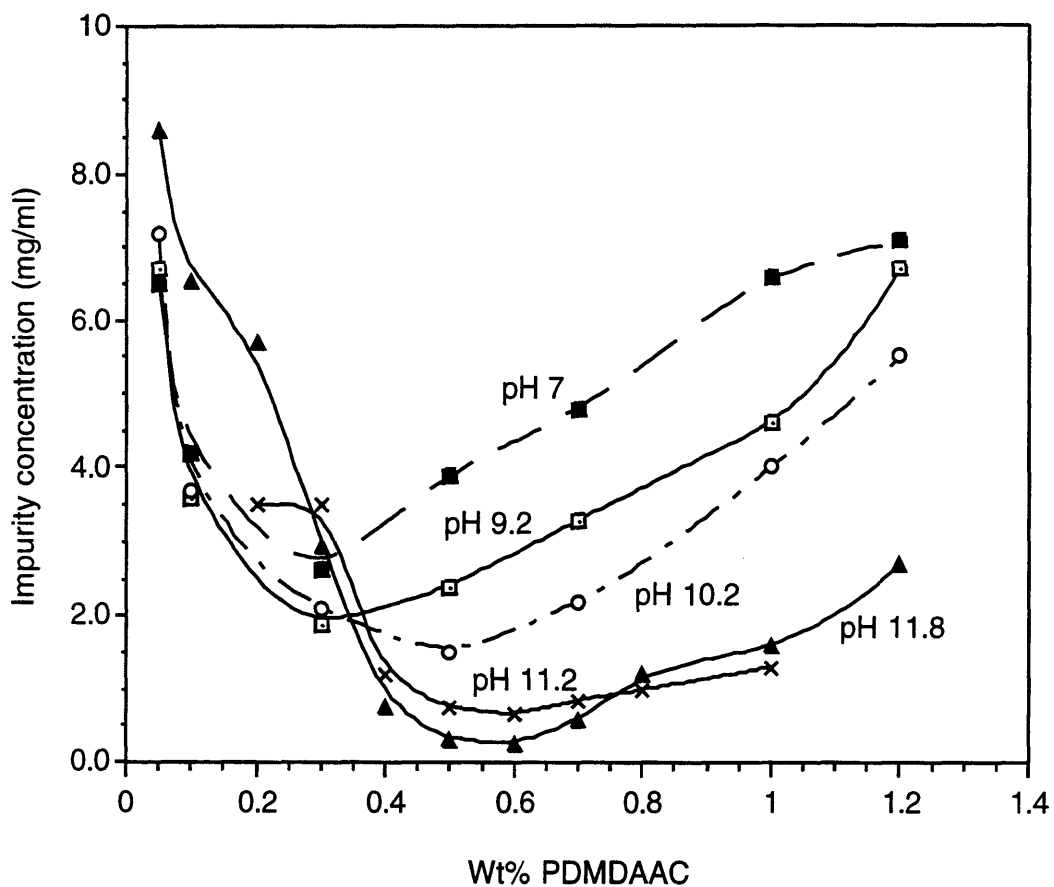


Table IV shows the effect of the different polymer treatments on SELP recovery. At a pH of 11.8, 22% of the SELP is lost during PDMDAAC precipitation compared with approximately 95% recovery at pH 8 for both the PDMDAAC and PEI treatment. This loss may be due to either isoelectric precipitation (salting-in) of SELP during the pH adjustment, or to complexation of the SELP (which becomes slightly anionic at this pH) to

the cationic polymer.

Table IV SELP8K Yields at Various Conditions

<u>Conditions for Polymer Flocculation</u>	<u>SELP Concentration in Supernatant (mg/ml)</u>	<u>SELP Yield (%)</u>
Untreated Lysate	2.05*	N/A
0.4 wt% PEI, pH 8	1.95	95%
0.3 wt% Merquat 100, pH 8	1.9	93%
0.6 wt% Merquat 100, pH 11.8	1.6	78%

*- untreated lysate diluted twofold for comparison purposes

Discussion: Further analysis of the PDMDAAC and PEI results yields insight on the mechanism of impurity removal. First, the level of impurity removal is influenced by the pH. For PEI precipitation, the concentration of protein impurities at optimal conditions ranged from 2.8 mg/ml to 2.2 mg/ml at pH 6.5 to pH 9 respectively, compared with an initial concentration of 8 mg/ml. This might be due to either more anionic compounds being present in the lysate at higher pH, or to a different

selectivity of PEI at higher pH, where the fractional ionization of PEI is significantly lower. A similar difference in impurity removal is observed between pH 7 and 9.2 (2.7 and 2 mg/ml respectively) for the PDMDAAC-treated lysate. Unlike PEI, PDMDAAC remains fully ionized at high pH, suggesting that the observed improvement in impurity removal at high pH is due to the presence of more anionic species capable of complexing with the cationic polymer. The ability of PEI to remove impurities from pH 8 to 9 does not appreciably improve, probably as a result of the few ionizable amino acids with pKa's in this range.

Adjusting the pH to 10 and greater converts more species in the lysate to anions. Cystine and tyrosine amino acid residues (pKa=8.3, and 10.9 respectively) become anionic and lysine residues (pKa=10.8) become neutral. Therefore, proteins containing these amino acids will exhibit improved polymer binding capabilities at high pH's. Above pH 10, more PDMDAAC is required to achieve the optimum impurity removal (0.3 wt% at pH 7 and 9 vs 0.6 wt% at pH 11.8), indicating that a greater fraction of the lysate is anionic at this pH.

The amount of PEI required to achieve optimal impurity removal also

increases with pH. This is due both to more anions being present in the lysate and to the lower fractional ionization of PEI at the higher pH. At a lower fractional ionization, more polymer is needed to complex a given amount of anionic impurities. The increased optimal PEI concentration at pH 8 compared with pH 9 is due primarily to a lower fractional ionization of PEI, since the level of impurity removal does not change appreciably. The effect of pH on the degree of ionization of PEI also has important ramifications on the separation properties of the resulting floc and is discussed next.

Solid-Liquid Separation: The ability of PEI to enhance the sedimentation of particles in the lysate is a major reason for its use. Table V shows a semiquantitative measure of the settling behavior for the solutions reported in Figure XIV.

Table V: Settling of PEI Treated Lysate, Measured by Visual Observation at 15 Minutes

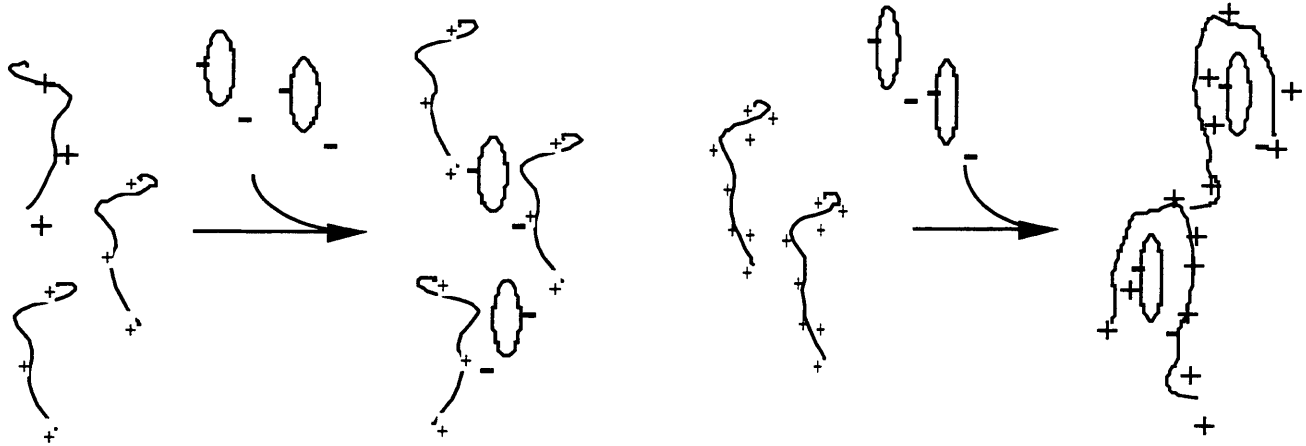
<u>Wt% PEI</u>	<u>pH 7</u>	<u>pH 8</u>	<u>pH9</u>	<u>pH10</u>
0.1	+	+		
0.2	++	++	++	++
0.3	++	+++	+++	++
0.4	+	+++	++++	++
0.5		++	+++++	+++
0.6		+	++++	++++
0.8			++	+++++
1.			+	++++
1.2				+++

The degree of settling is estimated after the PEI-lysate mixture has settled for 15 minutes. A greater number of plus marks indicates a faster relative rate of sedimentation. The maximal settling observed (pH 10, 0.8 wt% PEI) is approximately 50% of the initial volume. For a given pH, the optimal polymer concentration for settling corresponds closely with the optimal polymer concentration determined in Figure XIV for the removal of impurities. Thus, operating the precipitation process for optimal removal of impurities also results in near optimal floc-settling characteristics. This behavior is similar to that observed for the polymer flocculation of yeast, where settling rate also correlates with the yield of solids (Gasner, 1977). Results presented in Table V are from experiments at a small scale

(1 ml total volume), with fast mixing of polymer solutions and lysate. As mentioned in the background section, using data collected at this scale for the quantitative prediction of design parameters for centrifugal separation at large scale is tenuous. However, these data are useful for determining the effect of pH and PEI concentration on comparative settling behavior.

The greater degree of settling at higher pH can be explained by two scenarios. First the nature of lysate species that complex with the polymer is different at higher pH, resulting in a structurally different precipitate. The greater degree of impurity removal and setting exhibited by PDMDAAC precipitate at pH's above 11 is probably due to this mechanism. Another potential mechanism can also be invoked to explain the enhanced settling of PEI precipitates at higher pH. As illustrated in Figure XVI, a tradeoff between PEI wrapping around available anionic lysate species and those anionic lysate species serving to crosslink polymer strands is also consistent with the observed pH effect. At higher pH, larger floc sizes (as determined by settling rates) are observed because the mechanism depicted in Figure XVI (A) dominates over the mechanism shown in Figure XVI (B). At high pH, PEI is largely uncharged.

Figure XVI: Potential Mechanism of the pH Effect on PEI Flocculation



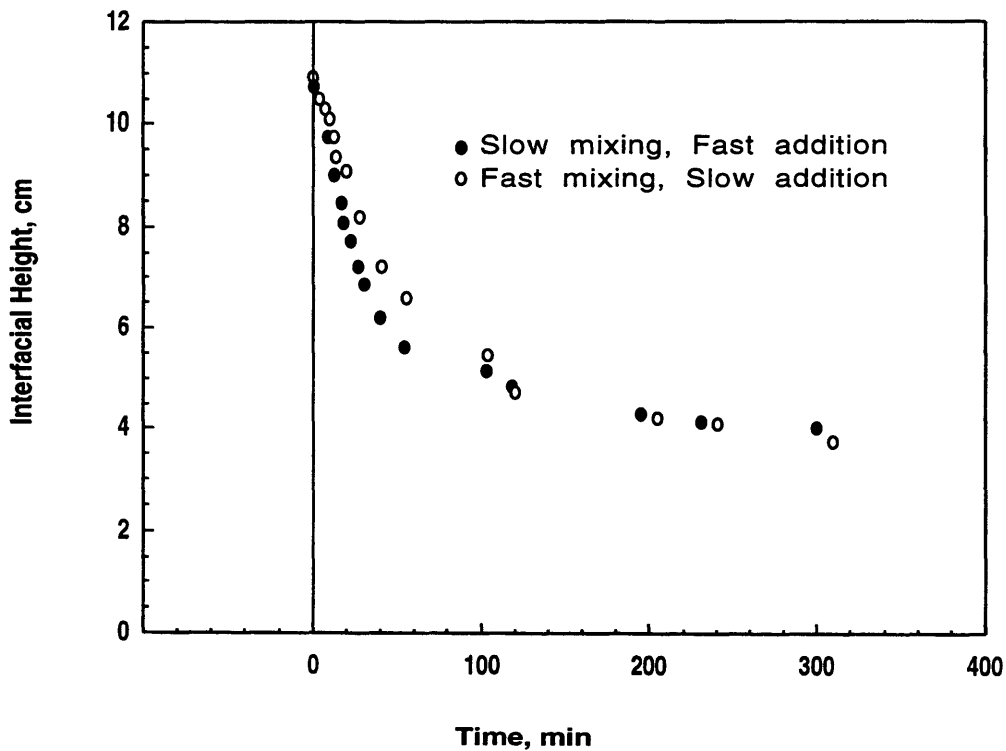
A. Polymer crosslinking: High pH, low PEI fractional, enhanced flocculation

B. Polymer wrapping: Low pH, High PEI fractional ionization, reduced flocculation

Thus, fewer and more spatially separated charge centers encourage a polymer-crosslinking mechanism over a polymer-wrapping mechanism. This analysis is suggested for systems with fast mixing and fast polymer addition rates: for instance small-scale batch contactors or large-scale static inline mixers. For systems exhibiting slow polymer addition rates, which are characteristic of large-scale batch processes, small nuclei will form first with additional polymer serving to bridge the smaller nuclei. Aging of the particles will occur during the polymer addition process. The final floc size and thus, separation characteristics, will probably depend primarily on the aging time and mixing rate (Bell, et. al., 1983).

To examine the effect of mixing and polymer addition rate on separability, a simple hindered settling test was used to determine the relative settling behavior of flocs produced by two extremes: a fast-mixing, slow addition rate case and a slow-mixing, fast addition rate case. The result, presented in Figure XVII, shows the suspension produced by fast addition, slow mixing to settle faster than the suspension formed by slow addition with fast mixing.

Figure XVII: Effect of Mixing and PEI Addition Rate on Settling Behavior.



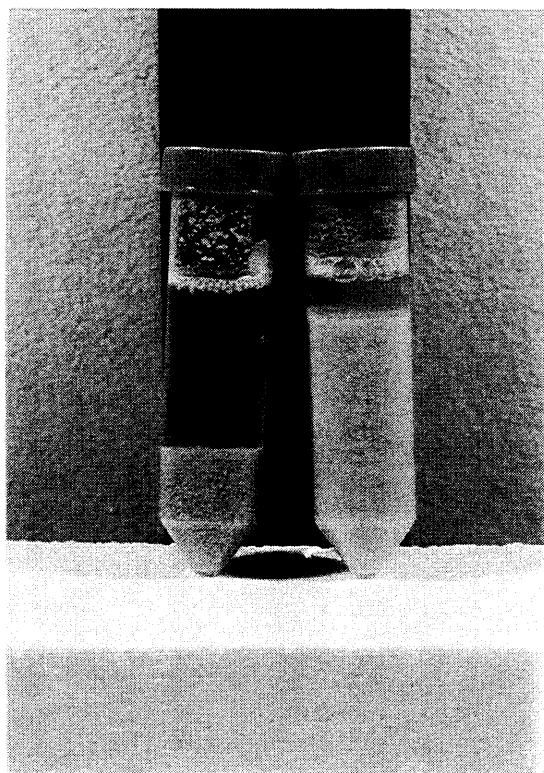
As previously mentioned, slow mixing with fast addition provides an

opportunity for large primary particles to form in localized zones of high polymer concentration, followed by aggregation of primary particles as the solution becomes mixed. Hindered settling tests are of limited value for predicting actual centrifugation performance as the high shear encountered in the feed zone of continuous centrifuges may degrade particles to smaller sizes (Bell and Dunnill, 1888). The differences in settling reported in Figure XVII are minor. Aging of the particulates in a shear environment, even during centrifugal separation, will probably minimize any difference in centrifuge performance between the two extreme cases presented above. Pilot scale experiments, with reactor geometries suggested in the next chapter, are desirable to determine an acceptable procedure for large-scale polymer precipitation and subsequent centrifugal separation.

The difference between the floc produced by PEI and PDMDAAC at the optimal conditions is illustrated by Figure XVIII. Lysate contacted with PDMDAAC solutions at pHs above 11 (left tube) forms large particles, with a characteristic size of approximately 1 mm. These particles settle very rapidly and have a coarse granular appearance that may be amenable to filtration, decanting, or cyclone devices for solid-liquid separation. The

PEI contacted solution is milky in consistency, with much slower settling properties as shown in Figure XVII.

Figure XVIII: Comparison of the Extent of Settling of Lysate Treated with PEI, and PDMDAAC Polymers at 20 minutes.



Ionic polymer precipitation does not result in total impurity removal. Soluble polymer-anion complexes are likely and will dissociate in the subsequent ammonium sulfate precipitation step, resulting in impurities

being carried through the process. This potential problem, and other scaleup issues, will be the focus of the next chapter. The following section will present results on the selective ammonium sulfate precipitation of SELP from the supernatant of the PEI precipitation process.

Ammonium Sulfate Precipitation: The next step in the purification process is to preferentially precipitate SELP. Two sequential ammonium sulfate precipitation steps are used for this purpose.

Effect of Temperature on Salting-Out Behavior: Figure XIX shows the salting-out behavior of prepurified SELP8K, SELP0K, and SELP0K-CS1 at room temperature (open symbols, solid lines) and 4°C (solid symbols, dashed lines). The data are plotted in the form of the Cohn equation (Equation one). Precipitation by salting-out is due to hydrophobic interactions, with the more hydrophobic species precipitating at lower salt concentrations. Thus, the order of increasing hydrophobicity of the three SELP species is SELP8K, SELP0K, and SELP0K-CS1. This order agrees with results of the hydrophobic interaction chromatography technique presented in Figure VII of Chapter IV and is the expected order obtained from inspection of the amino acid content of the different SELP species discussed in Chapter I. Operating at 4 °C shifts the salting-out curve for all SELP species to higher salt concentrations. This is expected as lower temperatures decrease hydrophobic interactions that drive precipitation by salting-out (Scopes, 1994). Parameters calculated for the Cohn equation, K (slope) and β (intercept), are shown in Table V.

Figure XIX: Effect of Temperature on the Salting-out Curves for SELP:
 ···▲··· SELP8K, 4⁰C; ···●··· SELP0K, 4⁰C; ···■··· SELP0K-CS1, 4⁰C;
 —▲— SELP8K; —○— SELP0K; —□— SELP0K-CS1.

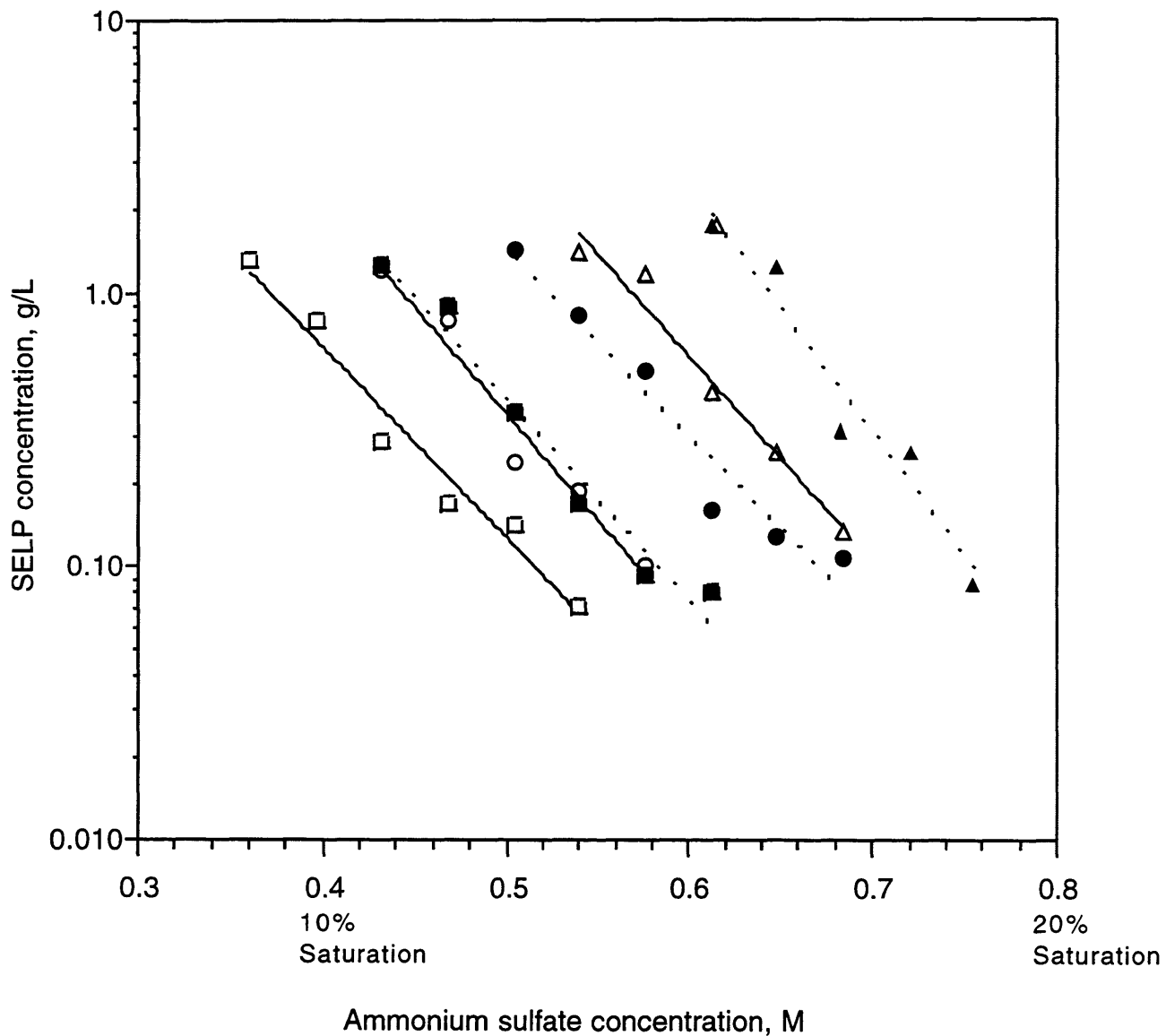


Table VI: Effect of Temperature on Parameters for the Cohn Equation:
 $\text{Log [S]} = \beta - K [\text{Salt}]$ for Different SELP species

	Room Temperature		4 °C	
	β	K, M^{-1}	β	K, M^{-1}
SELP8K	4.2	7.5	5.6	9.0
SELP0K	3.4	7.7	3.6	6.8
SELP0K-CS1	2.6	7.0	3.3	7.4

The observed values of K range from 6.8 M⁻¹ for SELP0K at 4°C to 9.0 M⁻¹ for SELP8K at 4°C. For comparison, a number of proteins listed in the literature have K's ranging from 2.8 to 7.8 M⁻¹ (Scopes, 1994; Melander and Horvath, 1977).

Temperature is expected to affect parameters of the Cohn equation in the intercept (β) and not the slope (K) (Melander and Horvath, 1977). As is expected, β did increase at the lower temperatures for all SELP species. The largest difference in K is for SELP8K, which change from 9.0 M⁻¹ at 4°C to 7.5 M⁻¹ at room temperature. This 15% difference is potentially due to experimental error resulting from variations in environmental

conditions. For instance, a temperature increase of approximately 40°C was observed during centrifugation of room temperature solutions, resulting in some samples remaining turbid after centrifugation. This may affect the value of the calculated K 's in a manner which is not consistent from sample to sample. Additionally, experiments on different SELP species were performed on different days, resulting in variations in the value of room temperature. Furthermore, ammonium sulfate concentrations were calculated by from the dilution of a saturated solution, and not by direct measurement. Errors in volumetric measurements could further introduce errors. As a result, these values should be used only for rough predictive purposes. A more systematic effort would be needed to determine the accuracy of the K and β values.

β is also expected to decrease at pH's nearer the isoelectric point (Melander and Horvath, 1977). No experiments were performed exploring this pH effect as the isoelectric point of SELP is above pH 9 where ammonium sulfate is no longer a suitable precipitant (Scopes, 1994). SELP is only weakly ionic, thus little effect of pH on salting-out is expected.

Effect of Lysate Impurities on SELP Solubility: The salting-out

curve of SELP from prepurified sources and from lysate is shown in Figure XX. Slope and intercept values are shown in Table VII.

Figure XX: Effect of Lysate Impurities on the Salting-out Curves for SELP:

···▲··· SELP8K, Lysate; ···●··· SELP0K, Lysate; ···■··· SELP0K-CS1, Lysate;
 —▲— SELP8K; —○— SELP0K; —□— SELP0K-CS1.

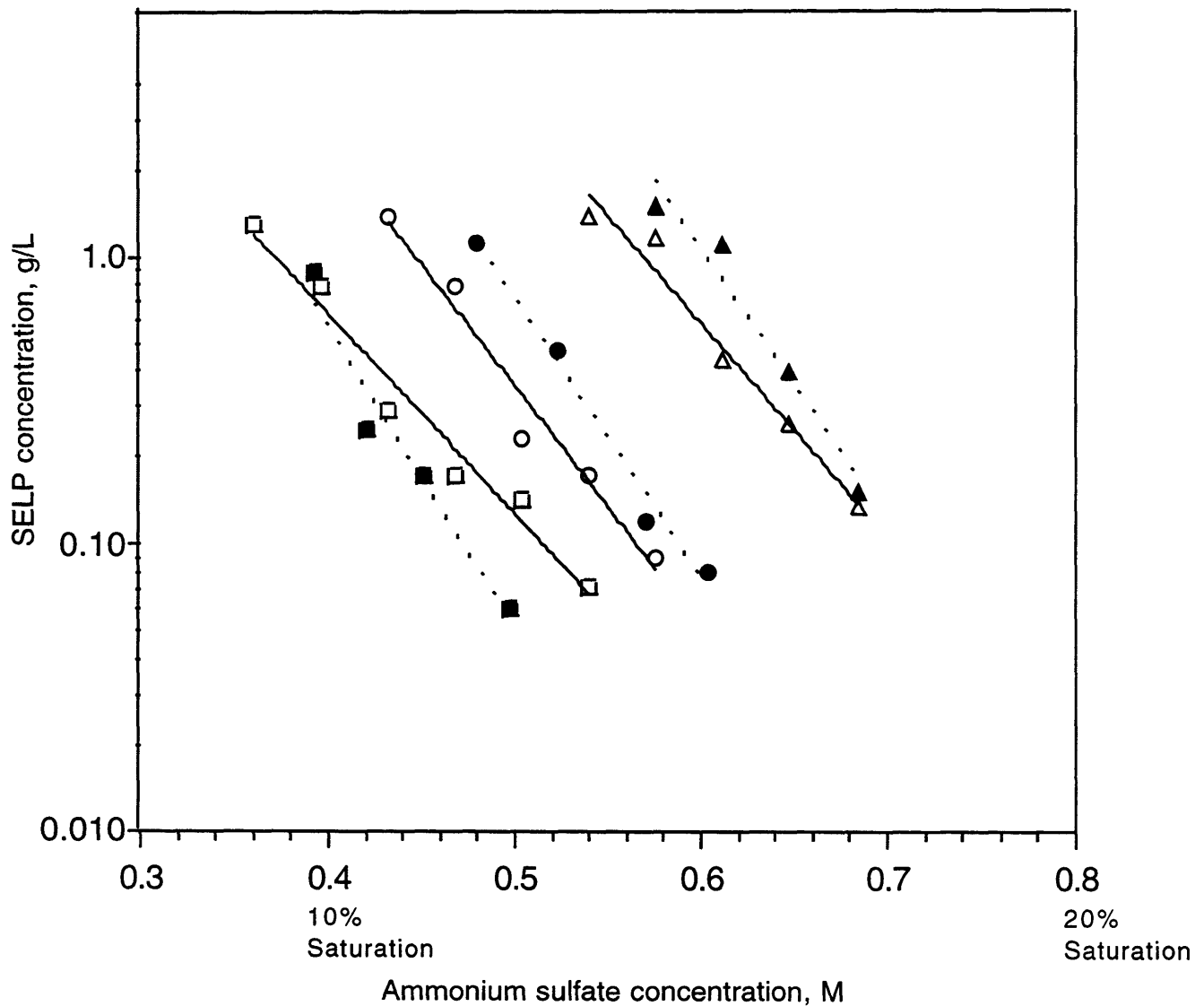


Table VII: Parameters for the Cohn Equation: $\text{Log}[S]= \beta - K [\text{salt}]$ for Different SELP Species Precipitated from the Supernatant of PEI Treated Lysate.

	<u>β</u>	<u>K, M^{-1}</u>
SELP8K	5.8	9.4
SELP0K	4.7	9.9
SELP0K-CS1	3.9	10.4

Slopes (K) for the lysate-derived SELP were consistently higher than slopes for prepurified SELP (shown in Table V). One reason for this may be that other compounds in the lysate may inhibit particle nucleation, which would show up as a shift of the data points at the lower degree of supersaturation to higher salt concentrations. Additionally, these solutions were obtained from a titration, i.e., by slowly adding saturated ammonium sulfate to the lysate and taking samples at discrete intervals. If solutions at the lower degree of supersaturation are not in equilibrium, then a larger slope would result. Experimental bias cannot be ruled out as an explanation of the observed differences.

The presence of impurities shifts the salting-out curve of SELP8K and

SELP0K-CS1 to higher salt concentrations. In contrast, the salting-out curve for SELP0K is shifted to lower salt concentration (except the data point at the lowest salt concentration). Reported literature on the effect of impurities on the salting-out behavior of proteins shows no consistent effect. Impurities shift the salting-out curve of rabbit muscle aldolase and pyruvate kinase to lower salt concentrations (Scopes, 1994). Scopes suggests this to be a general rule, but exceptions are noted such as with catalase, where the salting-out curve is shifted to higher salt concentration in the presence of impurities (Przybycien, 1994).

The chemical nature and concentration of impurities are expected to influence their effect on salting-out. As discussed in the next chapter, this may represent another scale-sensitive consideration as fermentation feedstocks are different at large scales, which may change the nature of impurities present in downstream processes.

Designing the precipitation operation requires specifying a final ammonium sulfate concentration. Given an expected SELP feed concentration of approximately 1 g/L SELP, adding enough ammonium sulfate to precipitate 99% of the SELP will result in a 0.01 g/L soluble

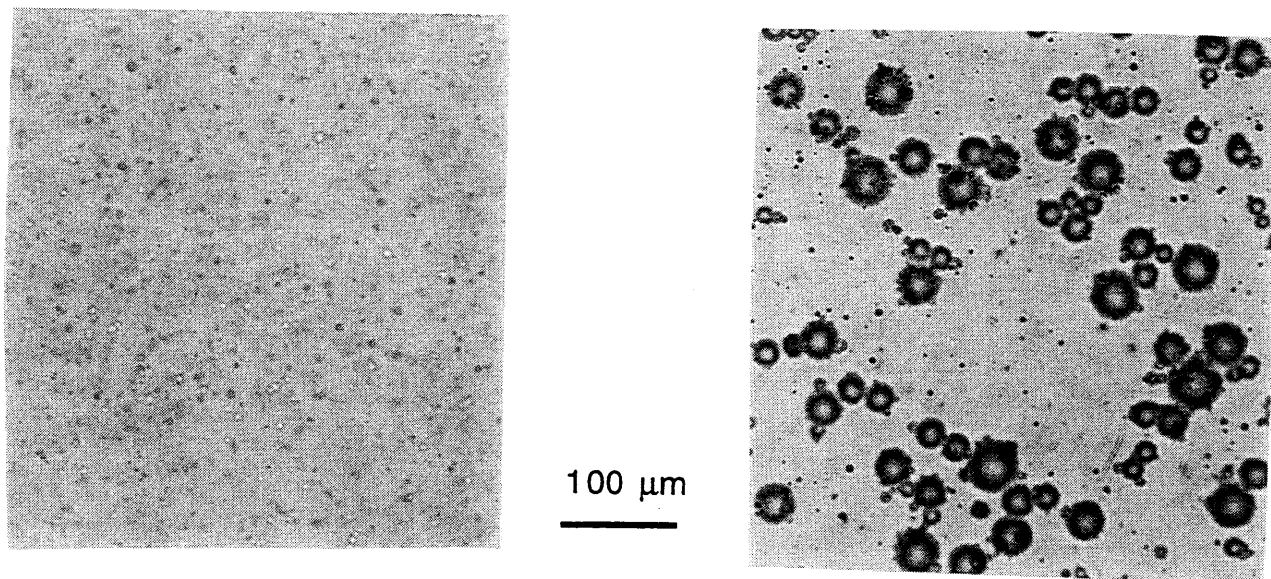
SELP concentration. The ammonium sulfate concentration needed to achieve 0.01 g/L soluble SELP concentration is calculated from the parameters listed in Table V. Thus for SELP8K, SELP0K, and SELP0K-CS1, the ammonium sulfate concentrations required are 0.83 M (20.5% saturation), 0.70 M (17.5% saturation), and 0.66 M (16% saturation), respectively. These values are for room temperature operations, which have the benefits of using less ammonium sulfate, and avoiding costly cooling operations. Drawbacks to room temperature operations potentially include an increase in protease activity and a different selectivity toward impurity removal. Should these concerns prove surmountable, room temperature operations are advantageous for economic reasons.

Characterization of SELP Particles: The actual yield of SELP through the precipitation process will depend on the separability of the particles, which is predominately determined by their size. Particle size is expected to depend primarily on the addition rate of the ammonium sulfate solution, and the mixing rate and extent of aging (Bell, et.al., 1983). These variables are highly scale-sensitive, and difficult to study at the small scales employed in this thesis. For these reasons, only a preliminary characterization of the effect that these variables have on particle size is

reported. As will be discussed in detail later, particles formed from SELP are more appropriately termed microdroplets, as they assume a spherical, highly deformable morphology. However, to maintain a consistent nomenclature throughout the document, the terms particle and precipitate are used to describe the phase separated product containing SELP.

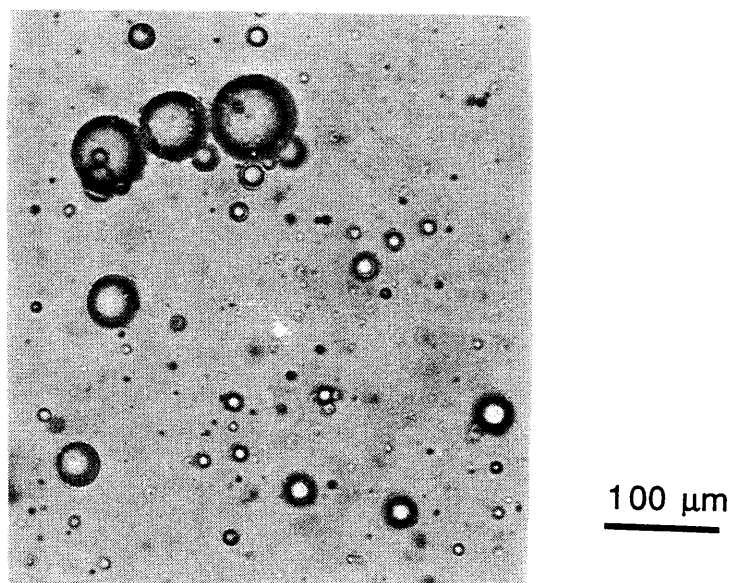
Figure XV (A & B) contrasts particles formed by two extremes: a fast precipitant addition and mixing configuration (characteristic of continuous tubular reactors), and a slow precipitant addition configuration (typical of batch or fed-batch reactors). Particles formed in the fast addition case are less than 10 μm in size, whereas those formed by slow addition are larger and more disperse in size, with sizes up to 50 μm seen. In a slow precipitant addition configuration, existing particles serve as surfaces for SELP to precipitate on as the concentration of ammonium sulfate is slowly increased. A quick mixing and precipitant addition configuration produces a fast solution change to high supersaturation resulting in rapid kinetics of nucleation, as illustrated in Figure VI (Chapter III). This results in a large number of small particles, which necessitates aging of the solution to increase particle separability.

Figure XXI: Morphology of SELP Particles from the Supernatant of Polymer Treated Lysate.



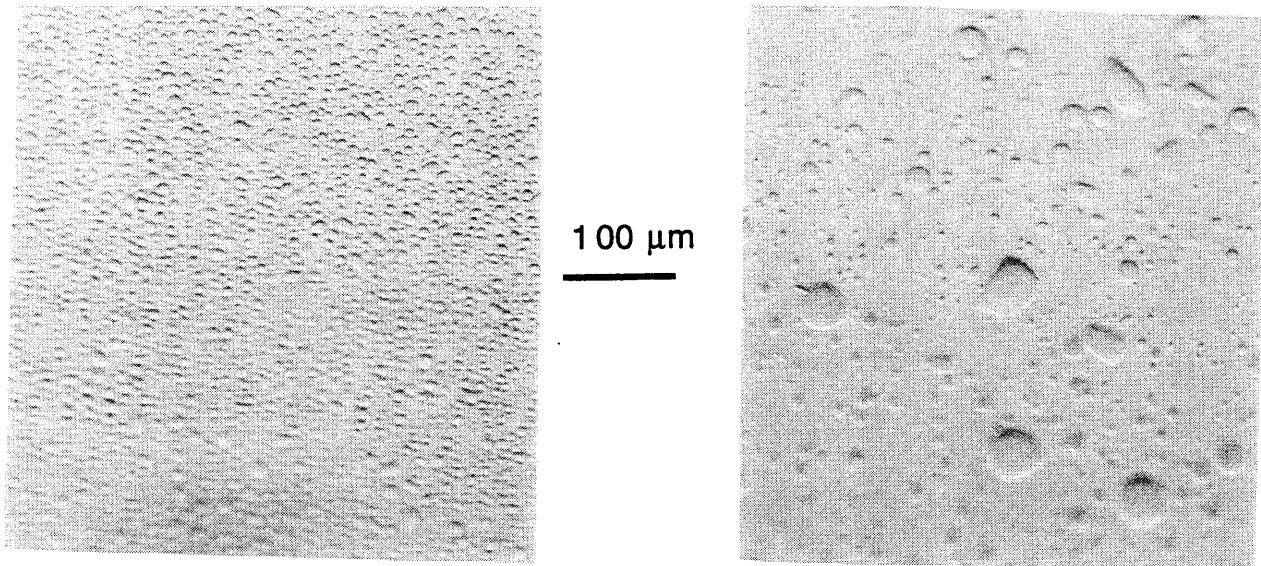
A: Fast precipitant addition

B: Slow precipitant addition



C: Fast precipitant addition with approximately 15 minutes aging

Figure XXII: Morphology of SELP Precipitates from Prepurified Sources.



A: Fast precipitant addition

B: Fast precipitant addition with aging

Figure XXI (C) shows that aging particles formed from a fast mixing configuration results in sizes similar to those formed in a slow addition configuration. Thus, continuous particle formation can give comparable results to batch particle formation if suitable aging of the particle is incorporated into the process. With aging processes, agitation time and rate influence particle aggregation and breakup mechanisms (Bell, et. al., 1983). These variables are strongly scale dependent, and should be determined at progressively larger scales.

Effect of Lysate Impurities on Particle Morphology: Figure XXII (A&B) shows particles formed from the second ammonium sulfate precipitation. Particles in Figure XXII (A) are formed from quick mixing and precipitant addition, whereas those shown in Figure XXII (B) are aged for approximately 5 minutes. Longer aging times result in yet larger particles which clump into large masses and tend to adhere to surfaces. Particles formed in the presence of lysate components resist adhesion and have a more spherical character, as shown in Figure XXI. This difference is suggested to be due to the presence of surface active agents in the lysate (proteins and other amphophilic molecules) which inhibit coalescence and adherence mechanisms.

All of the photographs in this section show that SELP precipitates form spherical microdroplets more characteristic of a second liquid phase than of a solid precipitate produced from a protein of known structure. For comparison, casein protein forms aggregates with irregular boundaries characteristic of a mechanism of fractal growth of primary particles (Bell, 1982). Slowly grown crystals of rabbit muscle aldolase and enolase are highly ordered with assignable crystal lattice geometries (Czoc, 1960). These proteins have singular structures enabling specific packing into a solid lattice. In contrast, the secondary or tertiary structure of

SELP is unknown. The primary sequence of SELP consists of blocks of the elastin repeat sequence (GVGVP) intermixed with the repeat silk sequence (GAGAGS). Native elastin has a helical structure, and native silk forms beta sheets with other nearby inter or intramolecular silk sequences. How these predisposed native structures impact the solution characteristics of SELP is not known. Size exclusion chromatography of SELP8K (Shown in Figures XI and XII) suggests the possibility of a mixture of monomeric and multimeric forms in solution. A previous report on keratin-myosin-epidermin-fibrinogen (KMEF) class proteins suggest that proteins which contain greater than three percent prolines by number, in the absence of crosslinks, are predisposed to adopt a random coil configuration (Szent-Gyorgyi, 1957). Roughly one in eight amino acids in SELP8K are prolines (12%), and an even larger proportion of prolines are present in SELP0K and SELP0K-CS1. Whether SELP in solution has some native structural elements of elastin and silk, or is a random coil, is uncertain. The morphology reported here shows that a heavy liquid phase is formed in ammonium sulfate solutions which is characteristic of a polymer with a large degree of flexibility in aqueous solutions.

The major determining factor in the ability to separate protein

precipitates is the size of the particles. Visual inspection of solutions at different aging times confirms that easily separable particles occur upon reasonable aging of the suspension. A more accurate designation of the operating conditions for particle aging should be determined at more industrially relevant scales. The adhesive nature of the particles formed during the second ammonium sulfate precipitation step poses potential processing challenges. Possible solutions to minimize this problem are proposed in the next chapter.

VI. PROCESS SYNTHESIS

A flowsheet on the process for SELP purification (starting at cell harvesting) is shown in Figure XXIII. An accompanying process flow diagram, with estimated material flows is shown in Figure XXIV. Material flows are estimated for input and output streams, based on a batch size of 10,000 L and an initial cell density of 50 g/L. For cells comprised of 50% protein, an initial SELP concentration of approximately 2.5 g/L or 25 kg/batch (10% total protein) enters the process. The amount of SELP in intermediate streams is listed, based on reasonable yield estimates. The process flowsheet is primarily based on a scaleup of the present small-scale laboratory process. When applicable, expected deviations due to scale-up are incorporated. These deviations are discussed later in this chapter. Processing notes and alternatives are presented in the two right-hand columns of Figure XXIII

Process design involves integrating individual unit operations to devise a viable process for large-scale production. Preliminary economic and technical evaluation at the expected final production scale are then used to decide which alternative technologies might be appropriate. These

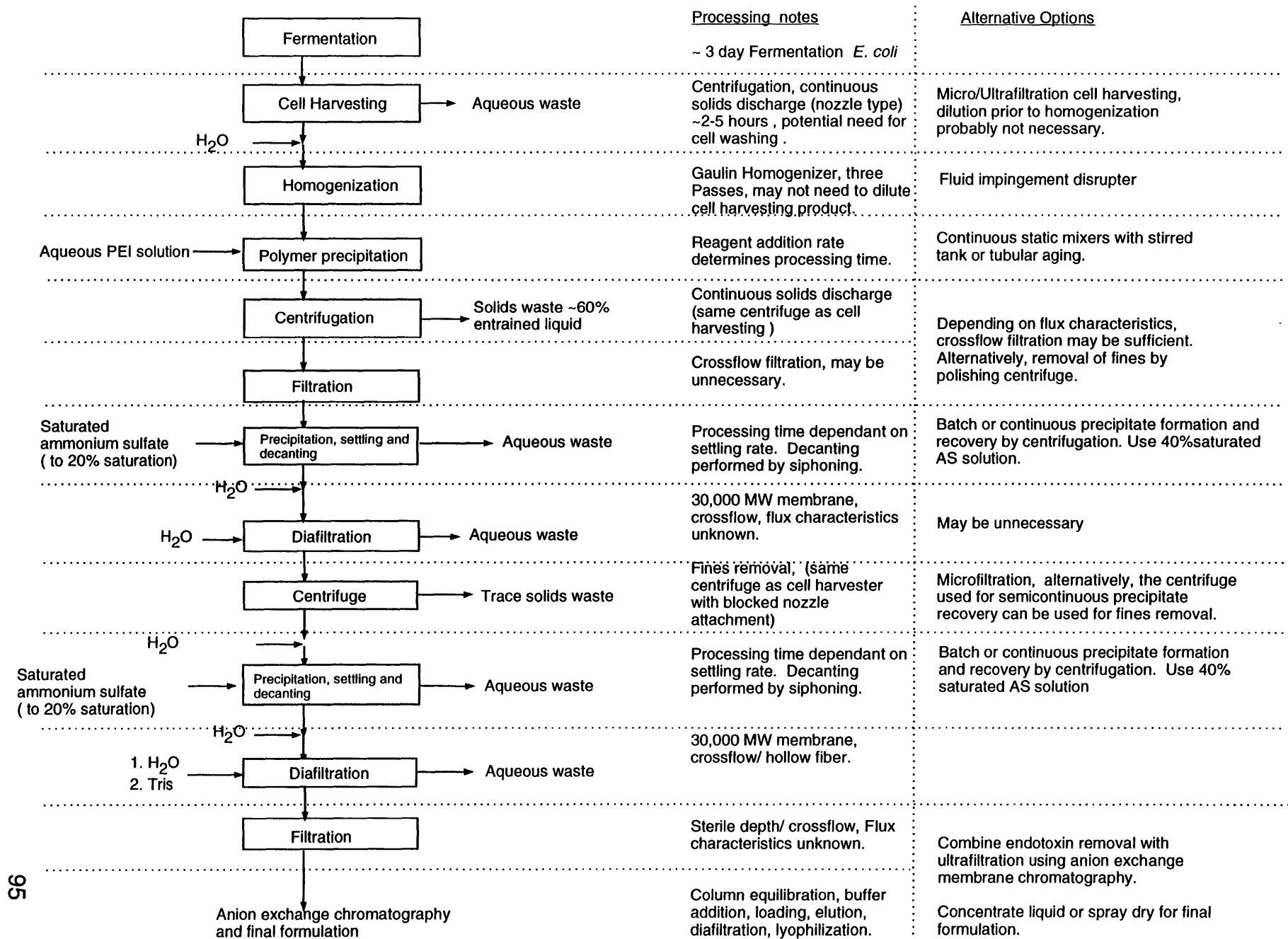
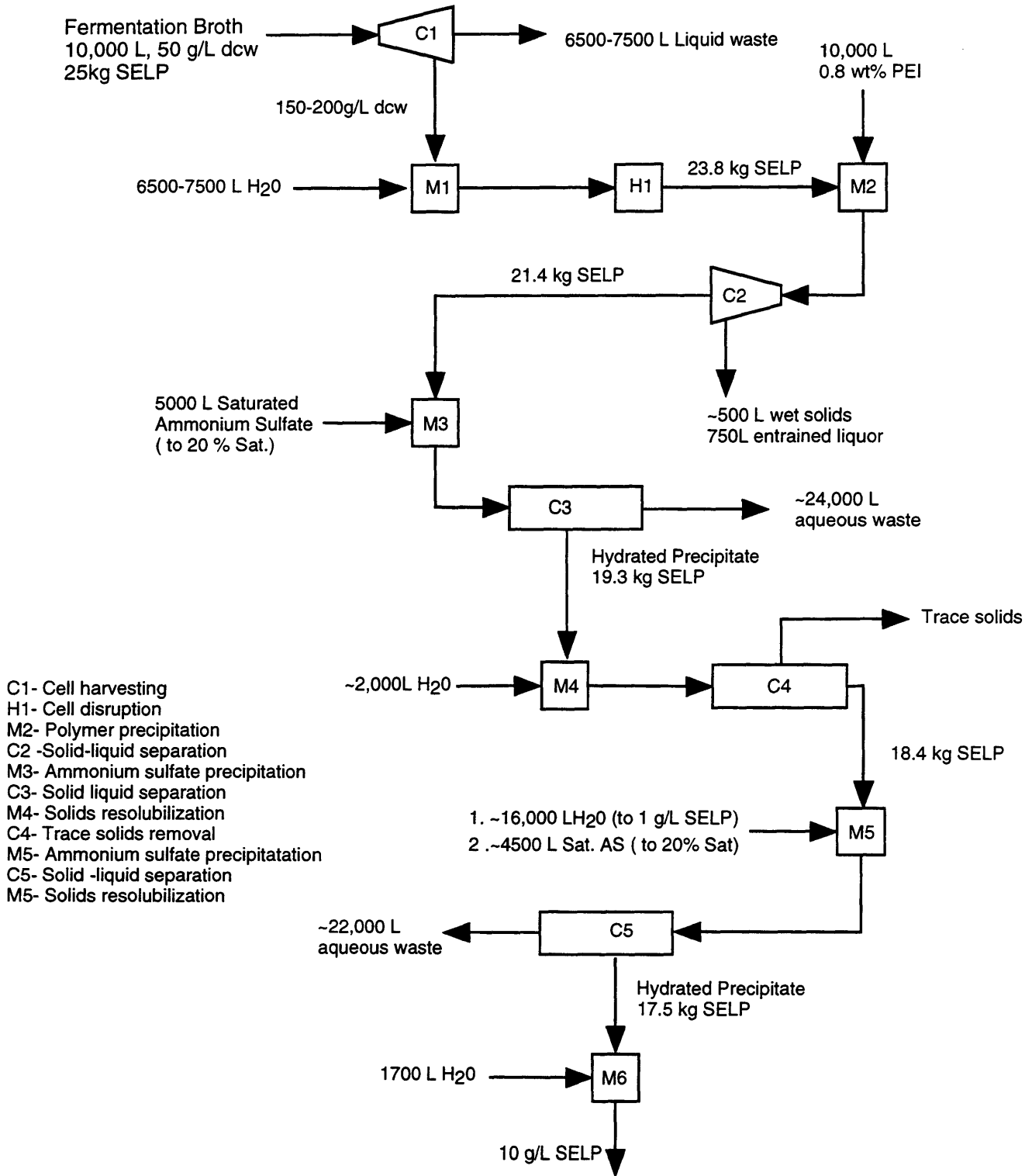


Figure XXIII: SCLP Purification Process Flowsheet

Figure XXIV: Process Flow Diagram for SELP Purification



- C1- Cell harvesting
- H1- Cell disruption
- M2- Polymer precipitation
- C2- Solid-liquid separation
- M3- Ammonium sulfate precipitation
- C3- Solid liquid separation
- M4- Solids resolubilization
- C4- Trace solids removal
- M5- Ammonium sulfate precipitation
- C5- Solid-liquid separation
- M5- Solids resolubilization

Intermediate product, on to buffer exchange, anion exchange
endotoxin removal, diafiltration, sterile filtration, and formulation

alternatives are technically evaluated at scales up to pilot plant size and the final design is chosen. This chapter incorporates results of prior chapters with general design strategies to provide a basis for choosing competing technologies for further evaluation. Also included in this chapter is a brief technical background for unit operations not previously covered in the introductory chapters.

Cell Harvesting: The first post-fermentation unit operation is cell harvesting. The continuous nozzle discharge centrifuge is the primary device used at large scales. A particulate slurry discharge consisting of 60-80% wet cells is typical for continuous centrifugation of *Escherichia coli* (personal communication, Rich Mathies, Alfa Laval Corporation). This corresponds to 120-180 g/L dry weight. Cell yields of >95% are common. SELP is an intracellular product and will end up in the particulate product of this operation.

A competing technology for cell harvesting is crossflow filtration. A comparison of costs associated with harvesting *Escherichia coli* showed that cross-flow filtration (Amicon 0.1 μm microporous membrane hollow fiber device, water removal rate = 5,000 L/hr) has a 70% lower capital

cost and a 25% lower operating cost than centrifugation (Tutunjian, R.S., 1985). This large difference makes one wonder why centrifugation is preferred for cell harvesting. Other than historic precedent, one reason may be that centrifuges are typically utilized for various tasks in the overall purification process, resulting in costs being spread over multiple process steps. Filtration equipment can also be used for multiple process steps, but high operating costs (due to membrane replacement) results in less savings than for centrifugation. One significant advantage of filtration is the absence of a workspace aerosol that is characteristic of centrifugal operations. Centrifugation is conducted in a contained environment when this is an important consideration.

Feedstocks used at large scales are typically molasses or corn steep liquor, both of which contain significant levels of impurities not present in the well-defined feedstocks used for small scale fermentations. Cell harvesting is an opportune time to remove these impurities.

Microfiltration allows for washing low molecular weight impurities from the cells, but high molecular weight compounds and small particles are retained. Cells can also be washed between successive centrifugation steps using a centrifuge equipped with a special nozzle discharge

mechanism that minimizes product loss due to premature cell lysis.

However, particles with similar settling characteristics to cells will be retained. For these reasons, the effect of feedstock variability on product quality should be assessed early in the design process and procedures implemented to handle expected feedstock-derived impurities.

Cell Disruption: Harvested cells are next disrupted to release SELP.

Both bead mill technology adapted from the paint and varnish industry and homogenization technology adapted from the dairy industry are utilized for industrial microbial disruption. Bead mills are most suitable for disruption of yeasts, mycelial organisms and microalgae, whereas high pressure homogenizers are more suitable for the disruption of bacteria and some yeasts (Engler, 1994).

The disruption of bacterial cells by high pressure homogenization can be accomplished by either valve type systems or fluid impingement systems. With a valve type system, such as the Manton-Gaulin APV, a cellular suspension is passed at high pressure through a specially designed spring loaded valve. Many different valve geometries are available, some with abrasion resistant ceramic surfaces for applications with bacterial

systems (Engler, 1994). The mechanism for cellular disruption is unknown, but it has been suggested that cells disrupt when exposed to the high shear associated with the impingement of high velocity fluid onto a solid surface (Engler, 1985). The large pressure drop occurring over a short time in these devices has also been suggested as causing cellular disruption, perhaps due to gases coming out of solution when the pressure is released (personal communication, Daniel I.C. Wang, MIT, 1996). Disruption in valve type devices exhibits first order dependence on the number of passes and power function dependence on the operating pressure, expressed as:

$$(4) \quad \ln(1-R) = -kNP^a$$

where R is the fraction disrupted, N is the number of passes, k is a rate constant which increases with temperature, and P is the operating pressure. For *Escherichia coli* grown in synthetic media, a value of 2.2 for the exponent a is reported for a Manton-Gaulin APV homogenizer (Engler, 1994). Disruption yields of 60-70% are typical in industrial operations, which necessitates multiple passes to achieve an acceptable yield. The high energy dispersion of these devices occurs as heat, which is removed

by heat exchangers between passes if product degradation is encountered.

Fluid impingement devices disrupt cells by impinging two portions of the process stream onto each other at high velocities. The relationship governing the performance of these devices is given by:

$$(5) \quad \ln(1-R) = -kN^bPa$$

The difference between the two devices, then, is that fluid impingement devices do not have a simple first order relationship with the number of passes. The exponent b varies with the specific growth rate and the type of cells being disrupted (Engler, 1994).

Cell concentration has little effect on the disruption efficiency of valve type homogenizers within the range of 30-170 g/L dry cell weight. As the cell harvesting centrifuge typically produces a slurry of 120-180 g/L, this slurry can be processed by the homogenizer without significant added dilution.

Polymer Precipitation: Design of the polymer precipitation operation

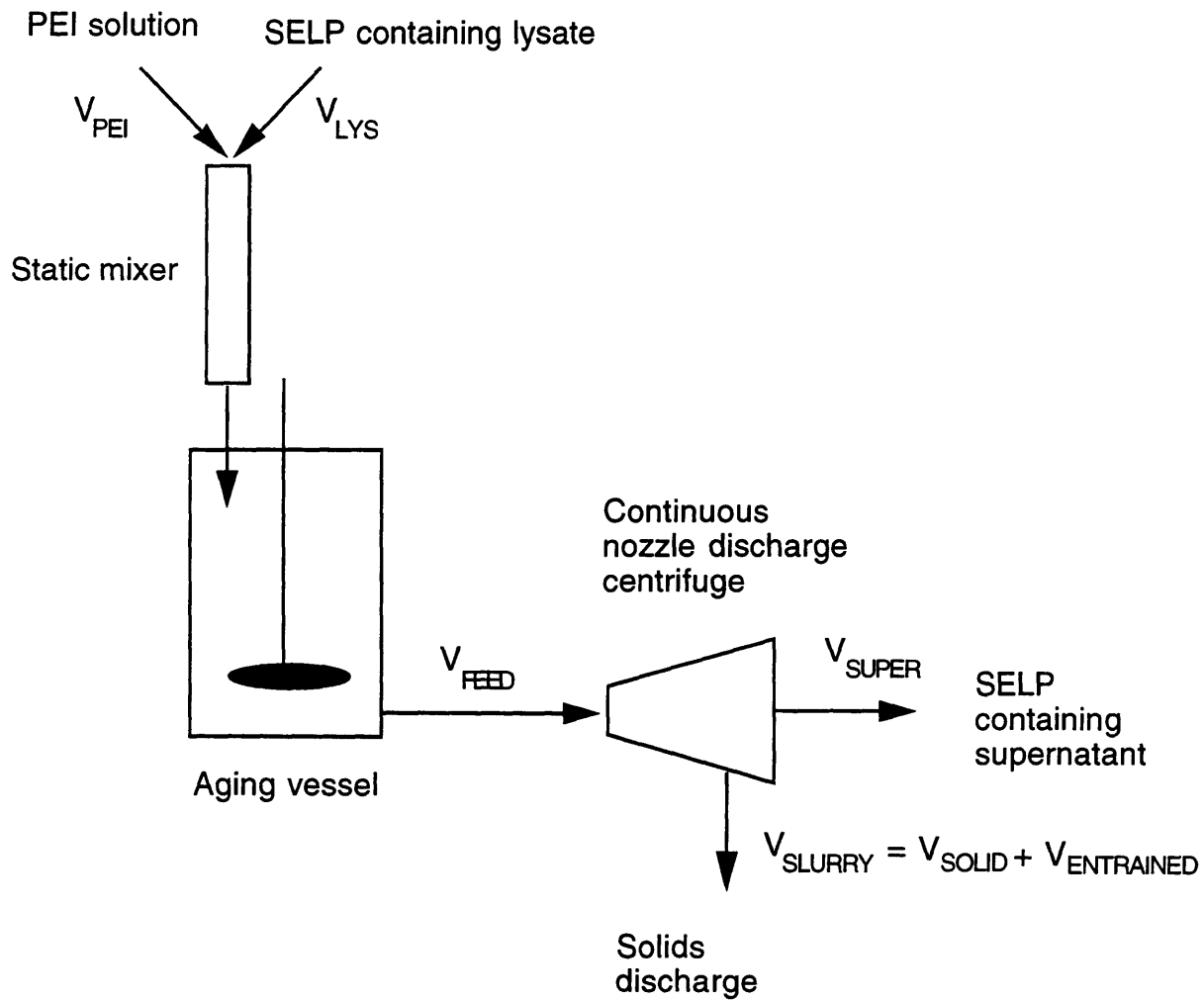
involves defining parameters associated with both impurity removal and solids separability. Parameters affecting impurity removal are the type and concentration of polymer and the pH. The effect of these parameters was shown in Figures XIV and XV. Both PEI and PDMDAAC treatment remove impurities with a similar efficacy at pH's between 7 and 9. When used above pH 11, PDMDAAC has significantly enhanced impurity removal properties over PEI. The disadvantage of using PDMDAAC at high pH is the handling of caustic solutions, and a potential loss of SELP (~5% loss was observed for SELP8K).

Precipitate removal efficiency is determined by the size, shape, and density of the particles. The type and concentration of polymer, as well as the pH, were shown in Table V, and Figure XVIII to have an impact on particle removal. PDMDAAC used above pH 11 produces a large granular floc which settles quickly, suggesting that gravity settling or filtration may be applicable for solids removal. Particles formed using PEI settle much slower than those formed using PDMDAAC, and are of a highly deformable nature. This indicates that filtration will not be a viable option for precipitate removal.

The effect of contacting mode on the settling rate of the PEI-produced precipitate was shown in Figure XVII. Settling rates of precipitates formed by fast PEI addition and slow mixing compared to settling rates of particles formed by slow PEI addition and fast mixing are comparable. This experiment bracketed conditions expected at large scales, suggesting that the mode of PEI addition can be designed on the basis of economic feasibility. Therefore, it is proposed that mixing of the lysate and PEI solution be accomplished with an inline static mixer, followed by a continuous stirred tank reactor for particle aging, and centrifugal separation using the same nozzle discharge centrifuge used for cell harvesting. This configuration is illustrated in Figure (XXV). This configuration has been tested at small scales, using a Gyrotester to quantify particulate removal, and produced a satisfactory product (personal communication, F. Ferrari, Protein Polymer Technologies, Inc.). As previously mentioned, the Gyrotester is a device which allows a prediction of commercial scale centrifuge performance. Aging of the particles may be needed to minimize particle disintegration in the subsequent centrifugation step. A CSTR aging vessel is shown in Figure XXV. Other particle aging schemes (discussed in Chapter III) may prove satisfactory. However, a variable volume aging vessel (CSTR) fulfills the

additional, potentially important, role of buffering fluctuations in the flowrate of the upstream polymer mixing and downstream centrifugation operations, resulting in a more robust process.

Figure XXV. Proposed Configuration for Polyethyleneimine Flocculation of Lysate



The yield of SELP through the PEI precipitation and subsequent centrifugal separation step is estimated using material balances on SELP (neglecting the SELP content of the solid) and on solids (neglecting changes of volume during mixing). This is expressed as:

$$(6) \quad \text{Yield} = 100 \cdot V_{\text{SUPER}} / (V_{\text{FEED}} - X_{\text{FEED}} \cdot V_{\text{FEED}})$$

where X_{FEED} is the volume fraction of solids in the feed to the centrifuge, and V_{SUPER} is given by:

$$(7) \quad V_{\text{SUPER}} = V_{\text{FEED}} - V_{\text{SLURRY}}$$

The balance on solids gives us the relationship:

$$(8) \quad V_{\text{SLURRY}} = X_{\text{FEED}} \cdot V_{\text{FEED}} / X_{\text{SLURRY}}$$

Where X_{SLURRY} is the solids content in the solids discharge stream.

Combining (8) and (7) with (6) and solving for the yield in terms of X_{FEED} and X_{SLURRY} gives the relationship:

$$(9) \quad \text{Yield} = 100 \frac{1 - X_{\text{FEED}} / X_{\text{SLURRY}}}{1 - X_{\text{FEED}}}$$

For the concentration of lysate and PEI used for this research, X_{FEED} was experimentally determined to be approximately 0.05. X_{SLURRY} is typically 0.4-0.6, i.e., the discharge mechanism of the centrifuge typically requires

40-60% entrained liquid for proper function (personal communication, Rich Mathies, Alfa Laval Corporation). Using a conservative value for X_{SLURRY} based on 60% entrained liquid results in a yield of 92%. As seen by equation (9) above, performing the precipitation from a more dilute solution decreases X_{FEED} , which increases the yield, at the cost of increasing the process volume. If the PEI precipitation is performed from a twofold more concentrated solution, then X_{FEED} is doubled and a yield of 83% is obtained. Optimal performance can be estimated by matching the cost of processing larger volumes to the increased value of the process stream due to higher yields.

Alternative technologies to centrifugation are filtration and gravity settling. Precipitates containing proteins are typically very difficult to filter due to a high filter cake resistance, or membrane plugging. If the flux characteristics of the filtration device prove acceptable, then filtration does allow for washing of the precipitate, which increases the SELP yield. For gravity settling, SELP yield depends on the liquid content of the settled solid. Figure XII shows that at near maximal settling (after approximately 3 hours), nearly 35% of the suspension volume settles with the solid phase. This represents a SELP loss of approximately 30%. The

entrained SELP is potentially recoverable by diluting the settled solids and allowing it to resettle, at the cost of processing greater volumes.

The decision to use PDMDAAC or PEI should be based on evaluating a tradeoff of operational benefits and concerns. The improved impurity removal observed with PDMDAAC at high pH should be weighed against the necessity of working with caustic solutions. Both PDMDAAC and PEI exhibit cytotoxicity, and hence must be removed by subsequent processing steps. The ability to validate removal of extraneous polymer by subsequent operations should also be considered in choosing which polymer to use.

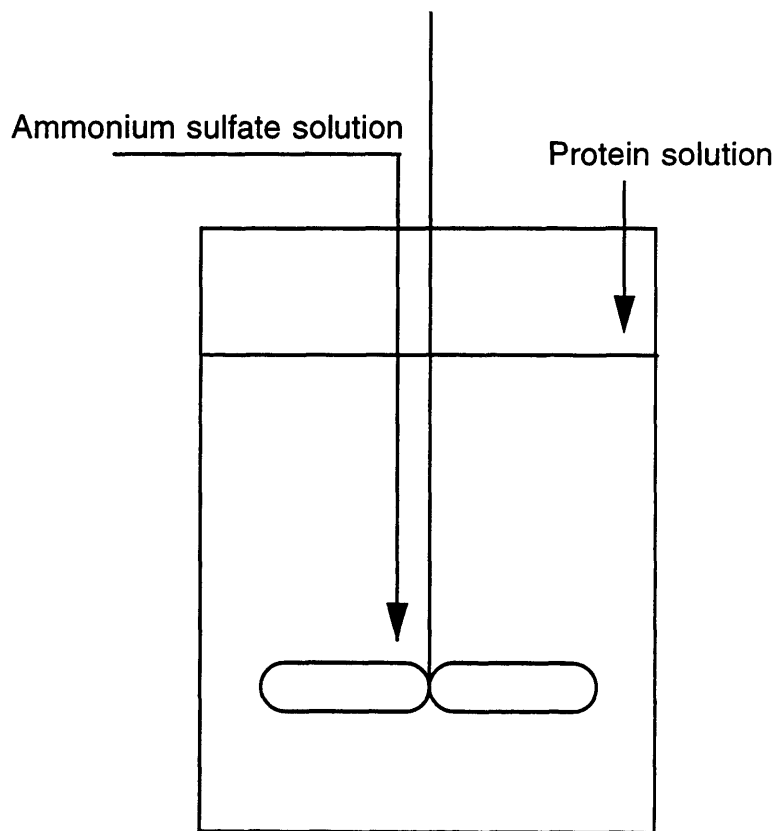
Currently, material of sufficient purity is being produced through the use of PEI. A continuous precipitation process with centrifugal separation using the cell harvesting centrifuge is proposed for large scale PEI precipitation. This configuration minimizes processing time and volume, and utilizes an underused centrifuge for fast solid-liquid separation, which provides significant economic advantages to batch process alternatives. Integration of this process with the subsequent ammonium sulfate precipitation process is discussed in the next section.

Ammonium Sulfate Precipitation: Both mixing rate and reagent addition rate are variables that strongly affect the separability of precipitates. As these variables are difficult to study at small scales, experimentation at progressively larger scales are necessary to confirm the design. Batch precipitation processes predominate at industrial scales. Typically the precipitant is sprayed across the surface of the solution, or sparged at the zone of high mixing to minimize overprecipitation of impurity proteins. The rate of precipitant addition influences both particle purity and separability, as discussed in Chapter III.

A potential improvement over batch configuration is fed batch, where the protein solution is fed at a zone of low mixing, and the precipitant fed at a zone of high mixing. The degree of supersaturation that the protein solution experiences is the most important variable for controlling particle size during the precipitation process (Iyer and Przybycien, 1994; Rothstein, 1994). Feeding the protein solution at a low mixing area of the tank utilizes the poor mixing characteristics of large scale operations to slow the rate of nucleation. Growth on existing nuclei will dominate in this setup, resulting in larger, more separable particles. This setup is illustrated in Figure (XXVI). Continuous operations can be realized using a

continuous stirred tank reactor (CSTR) for precipitate formation, followed by centrifugal recovery. Both fed batch and CSTR precipitators encourage growth on existing particles resulting in large, easily separable particles.

Figure XXVI: Fed Batch Precipitation Vessel



Continuous precipitation using static mixers, CSTR aging and centrifugation, similar to that proposed for the polymer flocculation operation (Figure XXV), has two additional advantages for recovering SELP precipitates. First, static mixers have very efficient and rapid mixing

capabilities, resulting in minimal overprecipitation of impurities. The second reason is due to the adhesive nature of the precipitates. A strategy of producing precipitates in near vicinity to recovery, and with minimal surface area, will minimize SELP losses due to nonspecific adsorption. Bell, et.al. (1983) report an estimate of relative reactor sizes for orthokinetic (shear induced) precipitation where pseudo-first order kinetics are assumed. A single CSTR needs 22 times the volume of a tubular plug flow reactor for equivalent performance. If three CSTRs are used in series, the required volume is lowered to 2.4 times the equivalent tubular reactor volume. Continuous particle formation in a tubular reactor minimizes volume requirements and hence minimizes adhesion losses.

The solid product from the centrifuge must be manually removed and solubilized for the next operation. Solubilizing the ammonium sulfate precipitate in the same stirred tank used for particulate aging would recover any material adhering to the aging tank. After dissolving the precipitate, the next operation is removal of insoluble impurities left over. The same centrifuge used for precipitate recovery is also appropriate for this step. Therefore, the same tank and piping network can be utilized for both operations, simplifying the operation and potentially recovering

adhered SELP.

The different SELP constructs have varying ammonium sulfate precipitation behavior, as reported in Chapter 4. However, at 20% saturation and room temperature, negligible soluble SELP remains for all constructs. As previously mentioned, the majority of *Escherichia coli* proteins are soluble at up to 40% saturation. Thus, using a 40% saturated ammonium sulfate solution as the precipitant, instead of a solid or saturated solution, will result in less overprecipitation of host proteins, and hence a potentially more pure product than if saturated ammonium sulfate is used. In order to examine the efficacy of this approach, tests were performed using the aforementioned Gyrotester in a continuous mixing, aging and centrifuge setup similar to that shown in Figure XXV. The result of these tests indicate that a continuous process using 40% saturated ammonium sulfate as a precipitant produces particles that are separable at high yields (personal communication, Franco Ferrari, Protein Polymer Technologies). Use of dilute ammonium sulfate solutions result in extra costs, due to greater processing volume, reagent costs, and waste disposal costs. However, the current knowledge regarding impurity removal is that the ammonium sulfate precipitation needs to be performed from a dilute

solution (<1 g/L SELP) to produce cytotoxin free product. Continuous particle formation, aging, and centrifugal separation would minimize extra costs associated with this necessary dilution of the process stream.

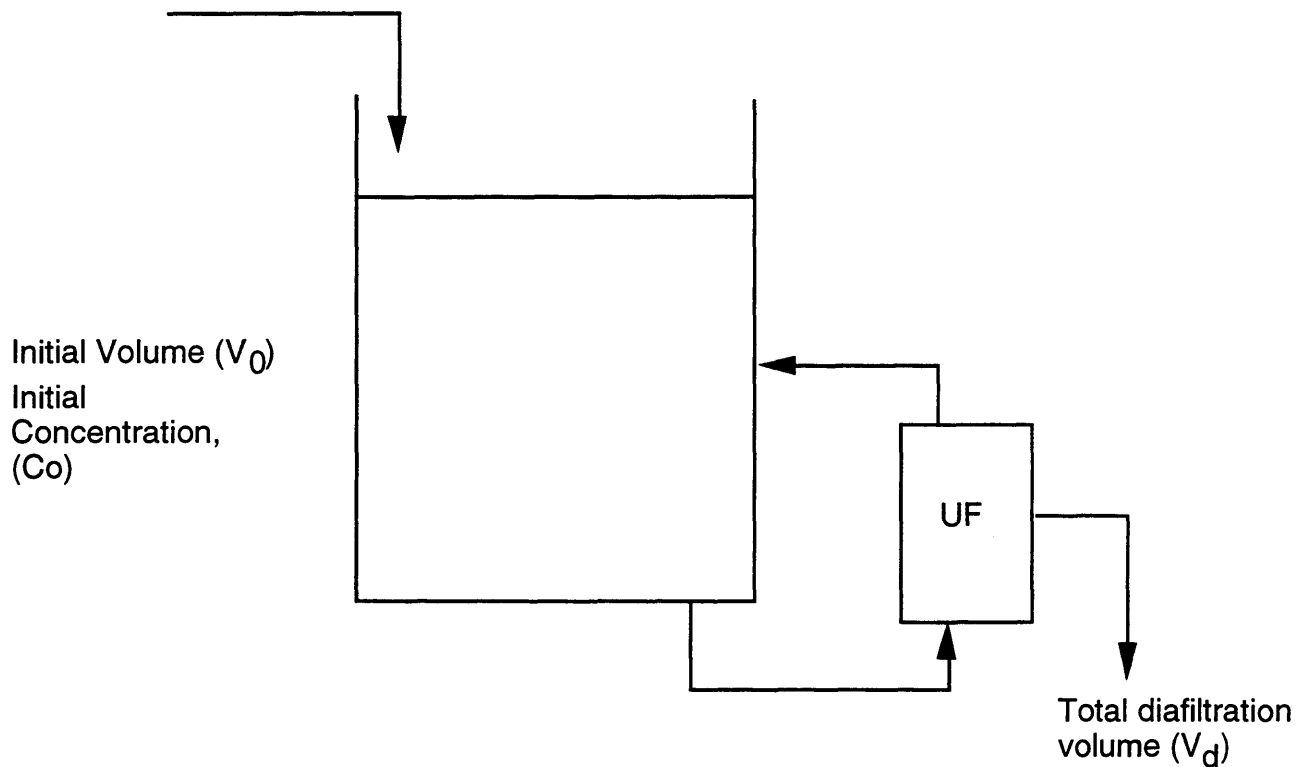
Diafiltration/Ultrafiltration: Ultrafiltration and diafiltration are utilized at various points in the process to concentrate protein solutions and effect removal of low molecular weight species. A typical scheme for ultra/diafiltration is shown in Figure XXVII below. For concentration purposes, the feed stream flowrate is set equal to zero. For diafiltration, typically the volume in the reservoir is held constant by equating the feed of fresh solution (buffer or water) with the filtrate rate. During diafiltration, the concentration of species retained by the membrane is given by the relationship :

$$(10) \ln (C_s/C_{s0})= -(1-R)V_d/V_o \quad (\text{Tutunjian, 1985})$$

where C_s is the concentration of impurity in the final solution, C_{s0} is the concentration of impurity initially, V_d is the total diafiltered volume, and V_o is the initial volume. The rejection coefficient R indicates the degree that a specific compound is retained by the membrane. $R=1$ for completely retained compounds and $R=0$ for compounds unhindered by the membrane. Thus for a 90% reduction in concentration of a compound with a rejection

coefficient of zero ($C_s/C_{s0} = .1$), a ratio of diafiltered to total volume of 2.3 is needed. The processing time required is determined by the flux characteristics of the device, which must be experimentally determined, and the membrane surface area.

Figure XXVII: Schematic of a Typical Dia/ultrafiltration Operation



Endotoxin Removal: Endotoxins are phospholipid components of the *Escherichia coli* cell wall which elicit a pyrogenic response in humans at extremely low levels. The removal of trace amounts of endotoxins is

essential for any biomedical product. Anion exchange chromatography, using perfusive beads, is currently used to remove endotoxins from the process stream prior to final diafiltration and formulation. In addition, anionic impurities not previously eliminated from the process stream are removed during this step. An alternative technology to bead-based chromatography is membrane chromatography. This technique uses micro or ultrafiltration membranes which have binding sites (e.g., ion exchange moieties) attached to the membrane support matrix (Thommes and Kula, 1995). Membrane chromatography has yet to achieve widespread use, but has the potential of integrating filtration and endotoxin removal in a single processing step, resulting in capital and operating cost savings.

Product Formulation: The current process has as its end product, lyophilized SELP. To produce SELP at large scales (1 metric ton per year expected demand), the cost of lyophilization will dominate other process cost. Concentrated liquid and air-dried solid formulation are two less expensive alternatives that should be evaluated for technical feasibility.

VII. BIBLIOGRAPHY

Axelsson, H.A.C. **1985**. Centrifugation. In Comprehensive Biotechnology (ed. Moo-Young, M.). **2**: 325-366.

Bell, D.J., Dunnill. **1982**. Shear Disruption of Soya Protein Precipitate Particles and the Effect of Aging in a Stirred Tank. *Biotechnology and Bioengineering*. **24**: 1271-1285.

Bell, D.J., Hoare, M., Dunnill, P. **1983**. The Formation of Protein Precipitates and Their Centrifugal Recovery. in Adv. in Biochem. Eng./ Biotech. **26**: 1-72.

Bell, D.J, Dunnill, P. **1982**. The Influence of Precipitation Reactor Configuration on the Centrifugal Recovery of Isoelectric Soya Protein Precipitate. *Biotechnology and Bioengineering*. **24**: 2319-2336.

Belter, P.A., Cussler, E.L., Hu, W. **1988**. BIOSEPARATIONS: Downstream Processing for Biotechnology. Wiley and Sons. NY, NY.

Boehringer Mannheim. **1972**. Process for the Enrichment of Proteins. UK Patent GB 1298431.

Bradford, M. **1976**. A Rapid and Sensitive Method for the Quantitation of Microgram Quantities of Protein Utilizing the Principle of Protein-Dye Binding. *Analytical Biochemistry*. **72**: 248.

Burgess, R.R., Jendrisak, J.J. **1975**. A Procedure for the Rapid, Large-Scale Purification of *Escherichia coli* DNA-Dependent RNA Polymerase Involving Polymin P Precipitation and DNA-Cellulose Chromatography. *Biochemistry*. **14**: 4639.

Cappello, J., McGrath, K.P. **1994**. Spinning of Protein Polymer Fibers. In Silk Polymers: Material Science and Biotechnology. Eds: Kaplan, D, Adams, W., Farmer, B., Viney, C. ACS Symposium Series **544**: pp 311-327.

Cohn, E.J., Strong, C.E., Hughes, W.L. **1946**. Preparation and Properties of Serum and Plasma Proteins IV. A System for the Separation into Fractions of the Protein and Lipoprotein Components of Biological Tissues and Fluids. *J. Am. Chem. Soc.*, **68**: 459-475.

Dubin, P.L., Murrell, J.M. **1988**. Size Distribution of Complexes Formed between Poly(dimethyldiallyl ammonium chloride) and Bovine Serum Albumin. *Macromolecules*. **21**: 2291.

Engler, C., R. **1994**. Cell Breakage. In: Protein Purification Process Engineering ed. R.G. Harrison. Marcel Dekker Inc., NY. pp 37-55.

Fisher, R.R., Glatz, C.E. **1986**. Effects of Mixing During Acid Addition on Fractionally Precipitated Protein. *Biotechnology and Bioengineering*, **28**: 1056-1063.

Foster, P.R., **1994**. Protein Precipitation. In Engineering Processes for Bioseparations. Ed. Laurence R. Weatherley. Butterworth-Heinemann, Oxford, Great Britain.

Foster, P.R., Dickson, A.J., Stenhouse, A., Walker, E.P. **1986**. A Process Control System for the Fractional Precipitation of Human Plasma Proteins. *J. Chem. Tech. Biotech.* **36**: 461-466.

Foster, P.R., Dunnill, P., Lilley, M.D. **1976**. The Kinetics of Protein Salting Out: Precipitation of Yeast Enzymes by Ammonium Sulfate. *Biotechnology and Bioengineering*. **18**: 545.

Gasner, L.L. **1977**. Microbial Cell Recovery Enhancement Through Flocculation. PhD Thesis, Massachusetts Institute of Technology, Department of Nutrition and Food Science.

Glatz, C.E., Fisher, R.R. **1986**. Modeling of Precipitation Phenomena in Protein Recovery. in Separation Recovery and Purification in Biotechnology: Recent Advances in Mathematical Modelling. ACS Symposium Series #**314**: 109-120.

Harrison, R.G. **1994**. Preface in: Protein Purification Process Engineering ed. R.G. Harrison, Marcel Dekker Inc., NY.

Hill, R.R., Zadow, J.G. **1978**. The Precipitation of Whey Proteins with Water Soluble Polymers. *New Zealand J. Dairy Sci. Technol.* **13**: 61.

Hoare, M. **1982**. Protein Precipitation and Precipitate Ageing. Trans. I. Chem. E. **60**(2): 79.

Iyer, H.V., Przybycien, T.M. **1994**. Protein Precipitation: Effects of Mixing on Protein Solubility. *AICHE Journal*. **40**: 349-360.

Jendrisak, J., Burgess, R.R. **1975**. A New Method for the Large-Scale Purification of Wheat Germ DNA-Dependent RNA Polymerase II. *Biochemistry*. **14**: 4634.

Jendrisak, J., **1987**. The Use of Polyethyleneimine in Protein Purification. in Protein Purification: Micro to Macro. pp. 75-97.

Kaplan, D., Adams, W.W, Farmer, B., Viney, C. **1993**. Silk Polymers: Material Science and Biotechnology. ACS Symposium Series 544, American Chemical Society, Washington, D.C.

McIntosh, R.V., Stenhouse, A., Woolard, D., Foster, P.R. **1989**. Improvements in the Formation and Separation of Protein Precipitates. In Solid-Liquid Separation Practice III. *Inst..Chem. Eng.* **113**: 77-92.

Melander, W., Horvath, C., **1977**. Salt Effects on Hydrophobic Interactions in Precipitation and Chromatography of Proteins: An Interpretation of the Lyotropic Series. *Archives of Biochemistry and Biophysics*. **183**: 200-215.

- Nelson, C.D., Glatz, C.E. **1985**. Primary Particle Formation in Protein Precipitation. *Biotechnology and Bioengineering*. **27**: 1434-1444.
- Niederauer, M.Q., Glatz, C.E. **1992**. Selective Precipitation. In Adv. in Bioch. Eng./Biotech. (Ed. A. Fiechter) **47**: 159-188.
- Parker, D.E., Glatz, C.E., Ford, C.F., Gendel, S.M., Suominen, I., Rougvie, M.A. **1990**. Recovery of a Charged-Fusion Protein from Cell Extracts by Polyelectrolyte Precipitation. *Biotechnology and Bioengineering*. **36**: 467-475.
- Porath, J. **1992**. Immobilized Metal Ion Chromatography. *Protein Expression and Purification* **3**: 263-281.
- Przybycien, T.M., Bailey, J.E. **1989**. Aggregation Kinetics in Salt-Induced Protein Precipitation. *AIChE Journal*. **35**: 1779-1790.
- Rothstein, F. **1994**. Differential Precipitation of Proteins. In Protein Purification Process Engineering. (Ed. Roger Harrison) pp. 115-208.
- Scopes, R. **1994**. Protein Purification: Principles and Practice. Third Edition, Springer-Verlag, New York.
- Sulkowski, E. **1985**. Purification of Proteins by IMAC. *Trends in Biotechnology*. **3**: 1-7.

Tal, M., Silberstein, A., Nusser, E. **1980**. Why Does Coomassie Brilliant Blue R Interact Differently with Different Proteins?: A Partial Answer. *Journal of Biological Chemistry*. **260**: 9976-9980.

Tebbe, H., Lutkemeyer, D., Gudermann, F., Heidemann, R., Lehman, J. **1996**. Gentle Separation of Hybridoma Cells by Continuous Disc Stack Centrifugation. Submitted for publication.

Thommes, J., Kula, M.-R. **1995** Membrane Chromatography-An Integrative Concept in the Downstream Processing of Proteins. *Biotechnol. Prog.* **11**: 357-367.

Tutunjian, R.S. **1985**. Cell Separations with Hollow Fiber Membranes. In Comprehensive Biotechnology. (ed. Moo-Young, M.) **2**: 367-381.

Watt, J.G., Smith, J.K. **1971**. Plasma Protein Fractionation. *Process Biochemistry*. **6**(9): 29-32.